UNIVERSITEIT TWENTE & UNIVERSITY OF ABERDEEN

Water Particle Velocities under Shoaling and Breaking Waves

Bachelor Thesis

Hidde van den Broek

9-7-2015

UNIVERSITEIT TWENTE.

1 4 9 5

UNIVERSITY OF ABERDEEN

Foreword

I have written this thesis to conclude my bachelor, it is a closure to 3 years of civil engineering and a first step in a more specialised direction. At the very beginning of this thesis, I only knew I wanted to do something in the direction hydraulic engineering. Now that I have experienced working in that field I am not disappointed, it was very interesting working towards the conclusions reached in this thesis.

I have learned a lot in the weeks I have spent at the University of Aberdeen. My supervisors have introduced me to linear wave theory, which was a necessary basis for writing this thesis, and guided me along through the process of writing a professional thesis. I would like to thank my supervisors, Thomas O'Donoghue, Dominic van der A and Angels Fernandez Mora, for all the effort they put into helping me.

Abstract

Sea waves approaching the shore will change in shape as a result of shoaling and wave breaking. This change in shape is reflected in the near-bottom velocities and is an essential mechanism that drives nearshore sand transport. The goal of this thesis is to determine the level of accuracy of the Isobe & Horikawa (1982), Elfrink *et al.* (2006) and Ruessink *et al.* (2012) parameterisations to predict wave-generated near-bottom velocities as a function of the surface wave characteristics. The parameterisations are used to predict near-bottom velocities from measured wave conditions, and the predicted velocities are compared to the measured velocities. The experimental data come from recent experiments carried out in a large-scale wave flume facility as part of the *Sand Transport under Irregular and Breaking Waves Conditions* (SINBAD) research project. The goal of that project is to improve understanding of the near-bed hydrodynamics and sand transport processes occurring under large-scale irregular and breaking wave conditions, and to develop a practical model which incorporates these new understandings to better predict sand transport under waves. Better understanding of the parameterisations that will be tested in this report will contribute to the development of the practical sand transport model.

Analysis of the comparison of velocities predicted by the parameterisations and measured in the experiments shows that none of the three methods satisfactory predicts the near-bed velocities. The results have implications for current morphological models that use these parameterisations and for the development of a new practical sand transport model within the SINBAD project.

Table of Contents

List of Figures

List of Tables

1. Introduction

Coastal morphodynamic models used in coastal engineering practice rely on empirical parameterisations to determine the near-bed (so called “free-stream”) water particle velocities. Even though there are already exact ways of determining the free-stream velocity using complex numerical models, these models are currently too computationally demanding for practical purposes, meaning that morphodynamic simulations over the course of days or even longer and over large areas are not feasible. Parameterisations should provide information on the free-stream velocities, which is accurate enough to use for the sediment transport calculations. These parameterisations typically use the local water depth, bed slope, wave height and the wave period as input to determine the free stream-velocities. Finding out how well the parameterisations describe the velocities for a breaking wave situation holds important practical relevance, since accurate velocities are essential to properly predict sediment transport rates in the breaking zone.

Therefore, the main question to be answered by this thesis is: How well do free-stream velocities estimated using the parameterisations of Isobe & Horikawa (1982), Elfrink *et al.* (2006) and Ruessink *et al.* (2012) compare to the measured velocities as regular waves propagate up a slope, break on a breaker bar and propagate?

Sub questions to be answered in support of the main question are:

1. How do the free-stream velocities estimated using the parameterisations of Isobe & Horikawa (1982), Elfrink *et al.* (2006) and Ruessink *et al.* (2012) compare to each other as regular waves propagate up a slope, break on a breaker bar and propagate?
2. Does the measured data behave as expected by theory on wave breaking and does it behave realistically?
3. How well do the maximum and minimum free-stream velocities estimated using the parameterisations of Isobe & Horikawa (1982), Elfrink *et al.* (2006) and Ruessink *et al.* (2012) compare to the measured maximum and minimum velocities as regular waves propagate up a slope, break on a breaker bar and propagate?
4. How well does the skewness of free-stream velocities estimated using the parameterisations of Isobe & Horikawa (1982), Elfrink *et al.* (2006) and Ruessink *et al.* (2012) compare to the skewness of the measured velocities as regular waves propagate up a slope, break on a breaker bar and propagate?
5. How well does the asymmetry of free-stream velocities estimated using the parameterisations of Isobe & Horikawa (1982), Elfrink *et al.* (2006) and Ruessink *et al.* (2012) compare to the asymmetry of the measured velocities as regular waves propagate up a slope, break on a breaker bar and propagate?

The parameterisation proposed by Ruessink *et al.* (2012), is currently the most recently proposed parameterisation. It has already been extensively tested using field data for several wave types. It has however not yet been tested at high resolution across a steep (1:10) beach profile, which will be done in this thesis. Elfrink *et al.* (2006) will also be tested, because it is relatively recent and partly calibrated with the same data as Ruessink *et al.* (2012). Isobe & Horikawa (1982) has for a long time been used widely in coastal engineering practice and it is interesting to see how it compares to more recent parameterisations, therefore this one will also be tested.

Using the recently acquired data from the SINBAD experiments, free-stream velocities will be calculated using the parameterisations. The calculated values will then be compared to the measured velocities.

In the second chapter of this thesis the theoretical background will be explained, since this is necessary for performing a well substantiated research. A short explanation of linear wave theory will be followed by a more in-depth look at the parameterisations. This will create the foundation for the research performed in later chapters, the first sub question will be answered to do so. The third chapter describes the experiments performed in 2014 for SINBAD. A description of the research facility, the test conditions and the measurements, including the used instruments, is given. The fourth chapter will provide the measured data and the outcome of the parameterisations, which will be compared with each other and the results discussed. Finally a conclusion will be made on the accuracy of the parameterisations and which one fits the measured data the best.

2. Theoretical Background

The parameterisations which will be tested rely partly on linear wave theory and partly on empirical results. It is important to understand what linear wave theory is and a short explanation of this and how waves work will be given in this chapter, followed by an explanation of the parameterisations.

2.1. Linear wave theory

Waves occurring naturally are random and short-crested. For coastal engineering simulations however, design waves are used for practical reasons. A design wave is long-crested and has a fixed height and period. Linear wave theory is one of the most important theories for simulating these waves, because of its simplicity it is easily used in models and calculations. Linear wave theory predicts a sinusoidal wave shape as seen in Figure 2.1. Its strict applicable range is small and only applies to waves of low steepness and in a situation of high relative depth. It can however be used outside of that range, resulting in results that are often accurate enough to be used for practical purposes.

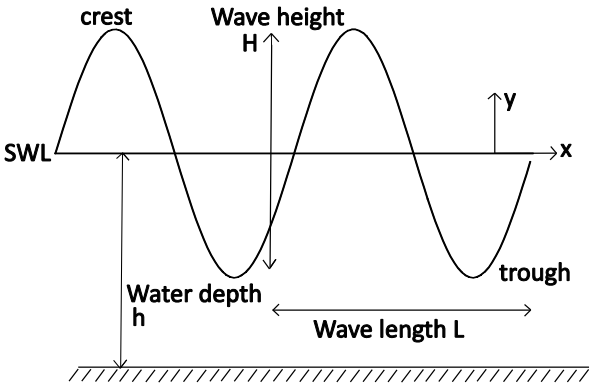

Figure 2.1: Definition sketch of wave parameters under a wave as predicted by linear wave theory

The velocity at which the water particles move is called the orbital velocity. With a given *H, T* and *h* the horizontal water particle velocity is given by

$$u = \frac{\pi H}{T}\frac{\cosh(k(y+h))}{\sinh(kh)}\cosh(kx - \sigma t) \tag{2.1}$$

and the vertical water particle velocity by

$$v = \frac{\pi H}{T}\frac{\sinh(k(y+h))}{\sinh(kh)}\sin(kx - \sigma t) \tag{2.2}$$

where *y* is the vertical position with *y* positive upwards from *y*=0 at the still water level (SWL) and σ is

$$\sigma = \frac{2\pi}{T} \tag{2.3}$$

where σ is the wave frequency and *k* is the local wave number and is given by

$$k = \frac{2\pi}{L} \tag{2.4}$$

The wavelength is calculated iteratively using

$$L = L_0 \tanh(kh) \tag{2.5}$$

where L_0 is the deep water wave length

$$L_0 = \frac{gT^2}{2\pi} \tag{2.6}$$

with *g* being the gravitational acceleration.

As can be seen from equation 2.1 and 2.2, water particles under a wave are driven by the free surface of the wave and vary with time. This makes the water particles move in an almost closed circular path. Under the crest they move in the same direction as the wave, under the trough they move slightly less in the opposite direction (Brown *et al.,* 2002). It results in a net movement of particles in the direction of wave propagation.

Near the bed, where *y*=-*h,* equation 2.1 is reduced to

$$u_0 = \frac{\pi H}{T \sinh(kh)} \tag{2.7}$$

u_0 is the near bed orbital velocity, also called the free stream velocity. In deep water, the orbital velocities decay exponentially, and u_0=0 (Abbot and Price, 1994). In shallow water however, the orbital velocities reach the bottom. Under influence of the seabed, the circular movement flattens out and becomes a to-and-fro movement parallel to and just above the seabed, the free-stream velocity (Brown *et al.* 2002).

Linear wave theory however does not produce good results for nearshore conditions. The shape of a wave is significantly different in the shoaling and breaking zone. As waves get to shallower water their height will increase according to

$$H_0/H = k_s = \sqrt{\frac{0.5L_0}{\frac{T}{c_g}}} \tag{2.8}$$

were c_g is group velocity at the inshore site and decreases when the waves get into shallower water; H_0 is the deep water wave height. Furthermore, the crest of the waves will become much shorter than the troughs. The margin of error in using linear wave theory under these conditions becomes unacceptable. Eventually the wave will become unstable and break. In this thesis the waves break in the form of the plunging type.

2.2. Skewness and asymmetry

Skewness and asymmetry are measures of the shape of the velocities and are important parameters that define the free-stream velocity. The velocity time series of a purely skewed wave is shown in Figure 2.2 (note that in this and subsequent figures two wave cycles are shown for clarity). As seen in the figure, the duration of the crest T_c, is shorter than the duration of the trough T_t. The maximum velocity in the crest is also higher than the maximum (negative) velocity in the trough. The measure of skewness of the wave is important, as skewed waves will drive a net sand transport.

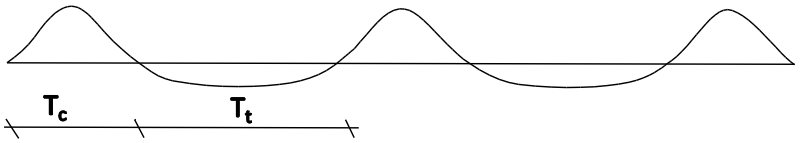

Figure 2.2: Velocity time series with skewness, velocity along the y-axis and time along the x-axis

The velocity time series of a purely asymmetric wave is shown in Figure 2.3. The time that the velocity is accelerating T_{ac}, is shorter than the time that the velocity is decelerating T_{dc}. So, an asymmetric wave has a higher positive acceleration than its negative acceleration.

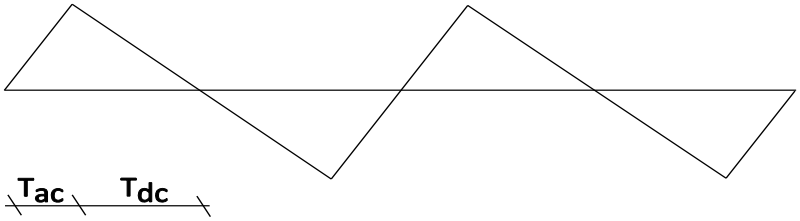

Figure 2.3: Velocity time series with asymmetry, velocity along the y-axis and time along the x-axis

The combination of both skewness and asymmetry creates a velocity time series as seen in Figure 2.4, this is how the free-stream velocity will look in a realistic wave.

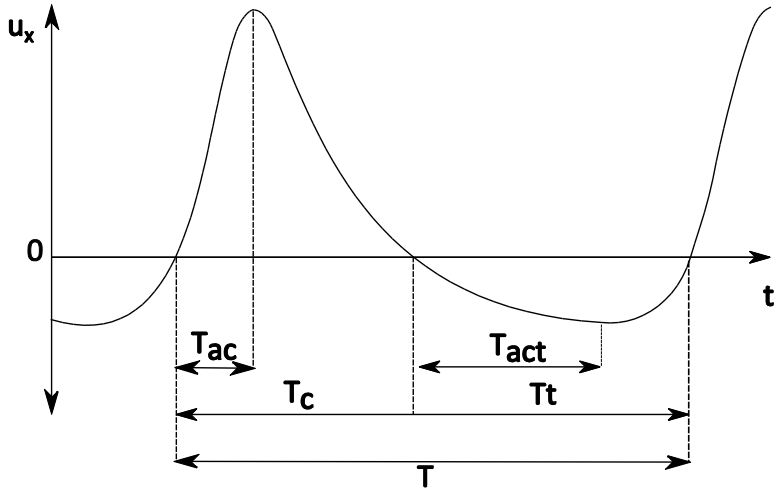

Figure 2.4: Wave with skewness and asymmetry, velocity along the y-axis and time along the x-axis, T_{act} is the acceleration in the negative x-direction, adapted from: Van der A *et al.* (2013)

The skewness can be calculated using

$$S_u = \frac{\overline{u_0^3(t)}}{\sigma_u^3} \tag{2.9}$$

where the crossbar indicates a time average and σ_u is the standard deviation of u_0. S_u=0 for a sinusoidal wave and S_u>0 for a skewed wave. A simpler measure of skewness that applies to regular waves is given by

$$R_{skew} = \frac{u_{max}}{u_{max} - u_{min}} \tag{2.10}$$

where u_{max} is the maximum value of u_0 and u_{min} is the minimum value of u_o. R_{skew}=0.5 for a sinusoidal wave and R_{skew}>0.5 for a skewed wave.

The asymmetry can be calculated with (Elgar, 1987)

$$A_u = \frac{\overline{H(u^3(t))}}{\sigma_u^3} \tag{2.11}$$

where H indicates the Hilbert transform. A_u=0 for a sinusoidal wave and A_u<0 for an asymmetric wave. For regular waves, a simple measure of asymmetry is given by

$$R_{asym} = \frac{a_{max}}{a_{max} - a_{min}} \tag{2.12}$$

where a is the flow acceleration. R_{asym}=0.5 for a sinusoidal wave and R_{asym}>0.5 for a skewed wave.

2.3. Parameterisations

Because linear wave theory fails in nearshore conditions, other theories like solitary wave theory were developed. Boussinesq or Reynolds-Averaged Navier-Stokes based models can make accurate descriptions of these shoaling processes. They are, however, too computationally demanding for practical purposes and because of that simpler parameterisations have been developed. Three of the most widely used ones will be discussed in the following sections.

2.3.1. Parameterisation of Isobe & Horikawa (1982)

The main equations of the parameterisation of Isobe & Horikawa (1982) are

$$u_0^{IH}(t) = u_c \sin\left(\frac{\pi t}{T_c}\right) \qquad for -\theta_2 T \le t < T_c - \theta_2 T \tag{2.13}$$

$$u_0^{IH}(t) = (\hat{u} - u_c) \sin\left(\frac{\pi(t-T) - \pi\theta_1 T}{T - T_c}\right) \qquad for\ T_c - \theta_2 T \le t < T - \theta_2 T \tag{2.14}$$

The parameterisation uses the water depth h, deep water wave height H_0, wave period T and the bed slope β as input.

Both equations describe the free-stream velocity for a certain period of the wave cycle. By combining two equations into one shape, it is easier to make a skewed and asymmetric velocity time series. However, the velocity at the points where the description of u_0 changes from the first equation to the second will show a discontinuity and the acceleration will show an unrealistic jump in height.

The full amplitude of the horizontal water particle velocity $\hat{u}$ is calculated using linear wave theory:

$$\hat{u} = 2ru_0 \tag{2.15}$$

r is a correction factor (the calculation of which can be found in Appendix A). u_c is given by

$$u_c = \hat{u}\left(0.5 + (B - 0.5)\tanh\left(\frac{A-0.5}{B-0.5}\right)\right) \tag{2.16}$$

where *A* and *B* are parameters (the calculation of which can be found in Appendix A). *g* is the gravitational acceleration and the calculation of λ_1-λ_4 can be found in Appendix A. T_c is calculated by

$$T_c = T\left(0.5 - (0.5 - D) * \tanh\left(\frac{0.5-C}{0.5-D}\right)\right) \tag{2.17}$$

where *C* and *D* is a parameter (Appendix A).

The parameterisations output was generated for the same input conditions given by Isobe & Horikawa (1982) to check whether it was constructed correctly. Figure 2.5 shows the output of the model, it corresponds well to the output shown in Isobe & Horikawa (1982).

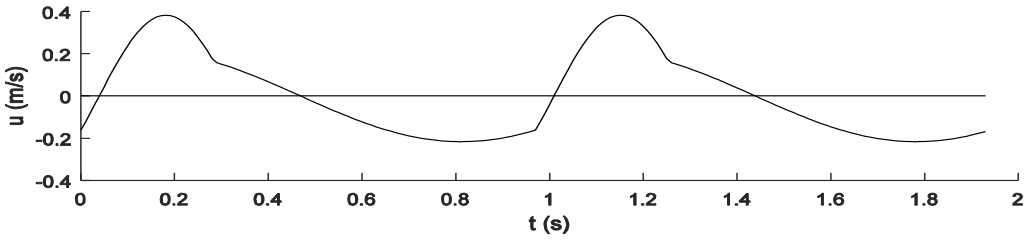

Figure 2.5: Graph produced by Isobe & Horikawa (1982), for H0/L0s=0.059, T=0.97s, h=0.104m

2.3.2. Parameterisation of Elfrink *et al.* (2006)

Elfrink *et al.* (2006) calculated the free-stream velocities under the crest, trough and the location (in time) of the zero crossings. A sinusoidal function was then adopted to describe the gaps between these calculated points. They define a normalised wave height given by

$$H^* = \frac{H}{h} \tag{2.18}$$

and a normalised wavelength given by

$$L^* = \frac{L}{h} \tag{2.19}$$

The parameterisation depends on the Irribarren number given by

$$\xi = \frac{\tan(\beta)}{\sqrt{\frac{H}{L_0}}} \tag{2.20}$$

Equations 2.21-2.24 define the near bed free-stream velocity:

$$u_0^E(t) = u_{max} \sin\left(\frac{\frac{1}{2}\pi t}{T_1}\right) \qquad for\ 0 < t < T_1 \tag{2.21}$$

$$u_0^E(t) = u_{max} \cos\left(\frac{\frac{1}{2}\pi(t-T_1)}{T_0-T_1}\right) - u_{0c} \sin\left(\frac{\pi(t-T_1)}{T_0-T_1}\right) \qquad for\ T_1 < t < T_0 \tag{2.22}$$

$$u_0^E(t) = -u_t \sin\left(\frac{\frac{1}{2}\pi(t-T_0)}{T_2-T_0}\right) \qquad for\ T_0 < t < T_2 \tag{2.23}$$

$$u_0^E(t) = -u_t \cos\left(\frac{\frac{1}{2}\pi(t-T_2)}{1-T_2}\right) \qquad for\ T_2 < t < 1 \tag{2.24}$$

u_t is equal to u_{min} but is always positive, T_0-T_2 determine the which part of the phase is described by which of the four equations and u_{0c} is a correction factor for the amplitude, these values are all calculated in Appendix B. Elfrink *et al.* (2006) is also discontinuous and therefore suffers from the same drawbacks already mentioned relating the discontinuity of Isobe & Horikawa (1982).

The parameterisation as a whole was scripted in Matlab and then verified with data from Elfrink *et al.* (2006). Figure 2.6 is output of the computed model for the same values Elfrink *et al.* (2006) described in their paper. Both figures are very similar to the figures seen in Elfrink *et al*. (2006), which leads to the conclusion that the parameterisation has been correctly implemented.

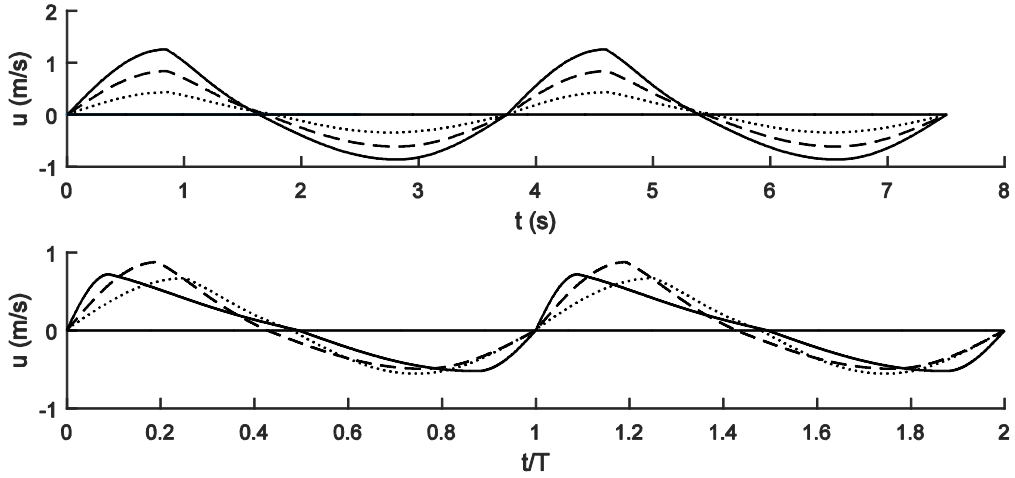

Figure 2.6: Elfrink *et al.* (2006) top figure: For h=2m, L/h=15, bed slope=1/40, solid line: H/h=0.6, dashed line: H/h=0.4 and dotted line: H/h=0.2 ,bottom figure: For h=2m, H/h=0.4, bed slope=1/40, solid line: L/h=25, dashed line: L/h=10 and dotted line: L/h=5

2.3.3. Parameterisation of Ruessink *et al.* (2012)

The parameterisation proposed by Ruessink *et al.* (2012) for estimating the free-stream velocity is based on the analytical expression of Abreu *et al.* (2010), which incorporates both skewness and asymmetry. For estimating the free-stream velocity time-series Abreu *et al.* (2010) proposed the following expression:

$$u_0^R(t) = u_0 \frac{\sqrt{1-r^2} * sin\left(\frac{2\pi}{T}t\right) + \frac{r*sin\Phi}{1+\sqrt{1-r^2}}}{1-r*cos\left(\frac{2\pi}{T}t+\Phi\right)} \tag{2.25}$$

where r and φ are parameters that control the shape in terms of non-linearity and phase. Ruessink *et al.* (2012) formulated new expressions for determining the non-linearity parameter r, equation 2.28, and the phase Φ, is given by

$$\Phi = \frac{\pi}{2} tanh\left(\frac{p_1}{U_r^{R\,p_2}}\right) \tag{2.26}$$

where p_1=0.815 and p_2=0.672 and the Ursell number U_r^R is given by (Doering and Bowen, 1995)

$$U_r^R = \frac{3}{8}\frac{\mathrm{H}k}{(kh)^3} \tag{2.27}$$

r is given by

$$r = \sqrt{\frac{2b^2}{b^2+1}} \tag{2.28}$$

where b is

$$b = \sqrt{\frac{2B^2}{2\mathrm{B}^2+9}} \tag{2.29}$$

and *B* is

$$B = \frac{p_3}{1+\frac{p_4-logU_r}{p_5}} \tag{2.30}$$

p_3 is the magnitude of *B* for $U_r^R \rightarrow \infty$, p_4 is related to the deflection point, and p_5 is a measure of the slope (Ruessink *et al*., 2012). Ruessink *et al*. (2012) determined the following values of p_3-p_5: p_3=0.857, p_4=-0.471, p_5=0.297.

Thus, through equations 2.26 – 2.28, the non-linearity parameter *r* and phase *φ* are a function of the Ursell parameter only. Because of this, the model is only dependent on the wave height, water depth and the wave period. The lack of a dependency on the bed slope means that the waves will react the same way on a steep and flat bottom, which is a weak point of this parameterisation.

The parameterisation was scripted in Matlab, after which it was tested with values from Ruessink *et al.* (2011). The correct output is produced, when the described values for *φ*, *r* and u_0 are put into the model. With *T*=7s, *φ*=-π/4, *r=0.5* and u_0=1.2m/s, which is one of the conditions from Ruessink *et al.* (2011), the computed free-stream velocity over time will look as in Figure 2.7.

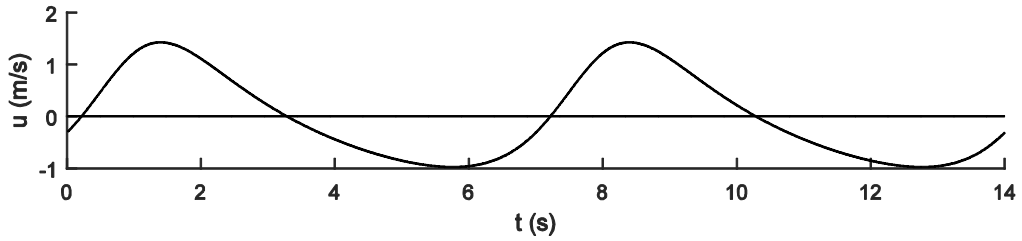

Figure 2.7: Estimated free-stream velocity over time, for *T*=7s, *φ*=-π/4, *r=0.5* and U_0=1.2m/s

2.4. Intercomparison of the parameterisations

Before the parameterisations are compared to the measured data, they will first be compared to each other in order to answer the first sub question. Figure 2.8 shows the three parameterisations for different values of *T*, the *h* and *H* remain constant.

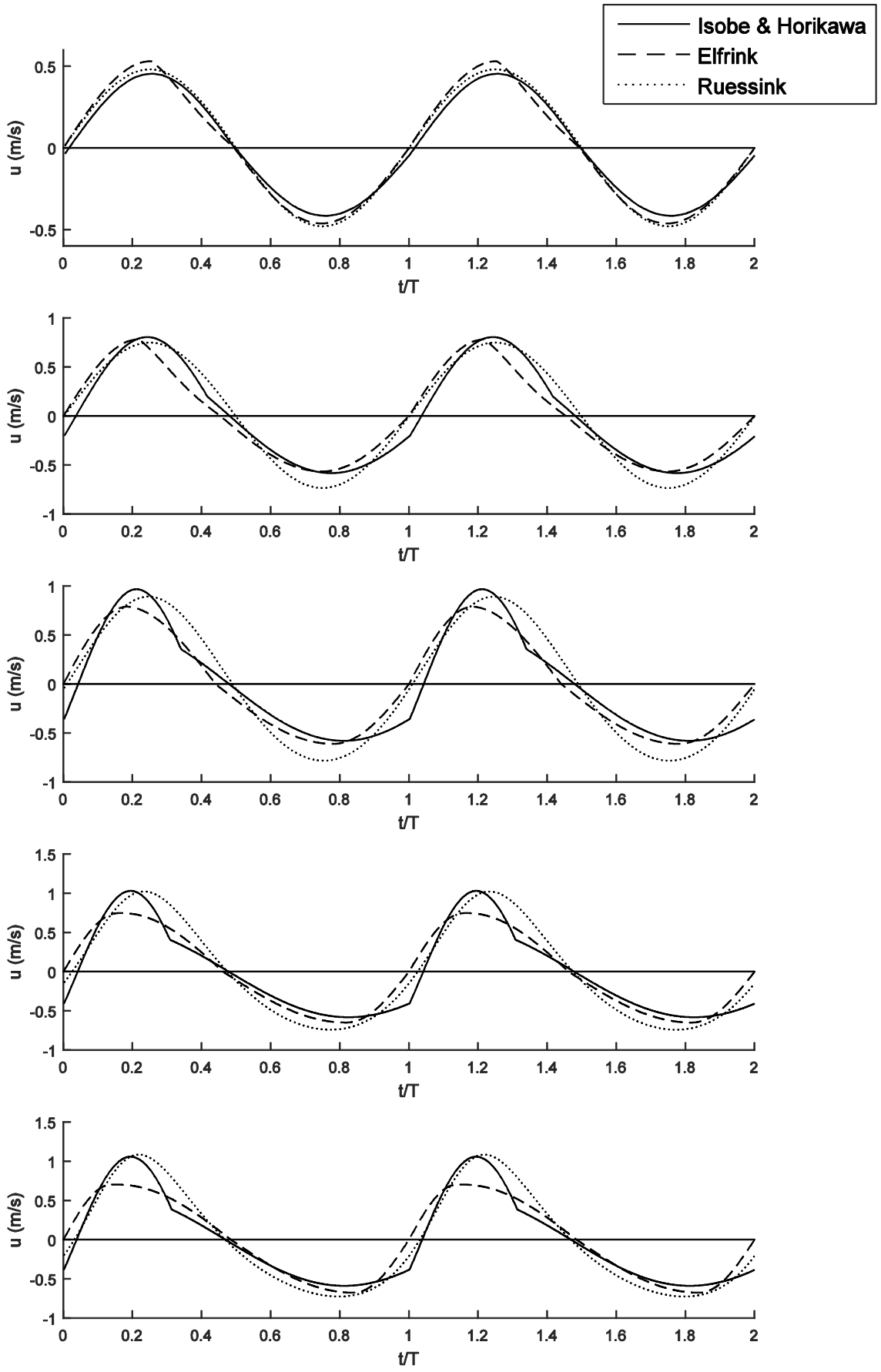

Figure 2.8: Near-bed orbital velocities predicted for *h*=1.5m, *H*=0.75m, from top to bottom: *T*=2, 3, 4, 5, 6s, solid line: Isobe & Horikawa (1982), dashed line: Elfrink *et al.* (2006) and dotted line: Ruessink *et al.* (2012)

Isobe & Horikawa (1982) and Ruessink *et al.* (2012) are clearly most sensitive to a change in the period; their maximum velocities differ a lot for changes in the period. It can also be seen that the maxima of all three parameterisations moves forward as the period becomes larger thus increasing asymmetry. Isobe & Horikawa (1982) and Ruessink *et al.* (2012) also show a rise in skewness; as the maxima become relatively bigger than the minima. The skewness of Elfrink *et al.* (2006) is highest at *T*=4s and lowest at *T*=6s, which is different to the behaviour of the other two parameterisations.

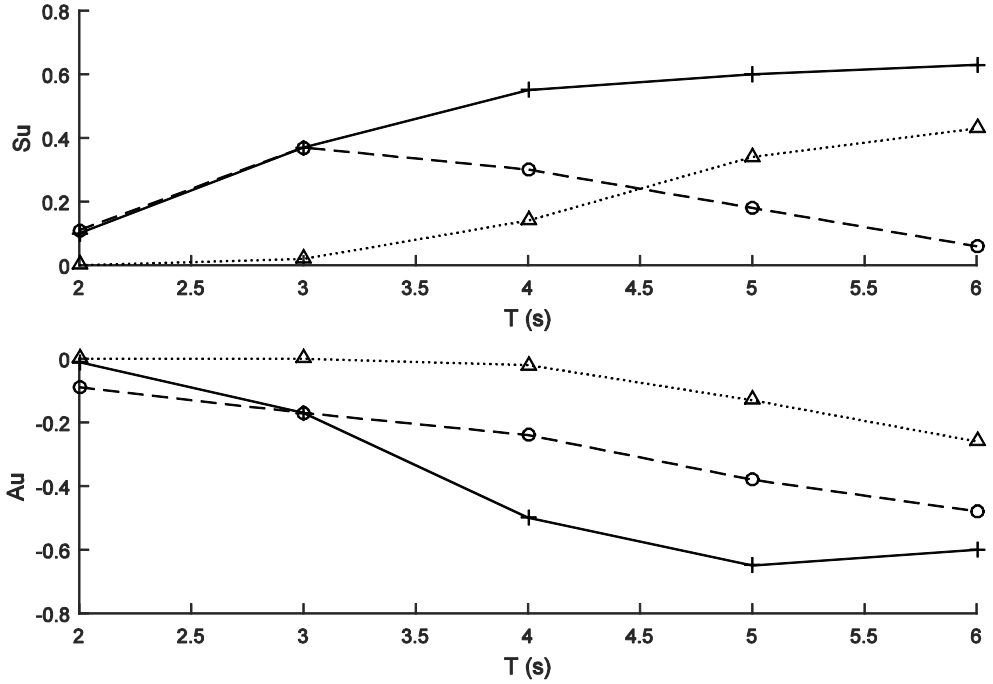

Figure 2.9: Top figure: S_u over T, bottom figure: A_u over T, plus (solid line): Isobe & Horikawa (1982), circle (dashed line): Elfrink *et al.* (2006), triangle (dotted line): Ruessink *et al.* (2012)

Table 2.1: Values of skewness and asymmetry depicted in Figure 2.9

	Isobe & Horikawa (1982)					Elfrink *et al.* (2006)					Ruessink *et al.* (2012)				
T (s)	2	3	4	5	6	2	3	4	5	6	2	3	4	5	6
Su	0.10	0.37	0.55	0.60	0.63	0.11	0.37	0.30	0.18	0.06	0.00	0.02	0.14	0.34	0.43
Au	-0.01	-0.17	-0.50	-0.65	-0.6	-0.09	-0.17	-0.24	-0.38	-0.48	0.00	0.00	-0.02	-0.13	-0.26

The figure shows clearly that the skewness and asymmetry increase for Isobe & Horikawa (1982) and Ruessink *et al.* (2012) as the period becomes bigger. Elfrink *et al.* (2006) has its maximum skewness at *T*=4 after which it decreases, its asymmetry increases over the entire length of the change in *T.*

Figure 2.10 shows the parameterisations for different values of the water depth, now the period and wave height remain constant.

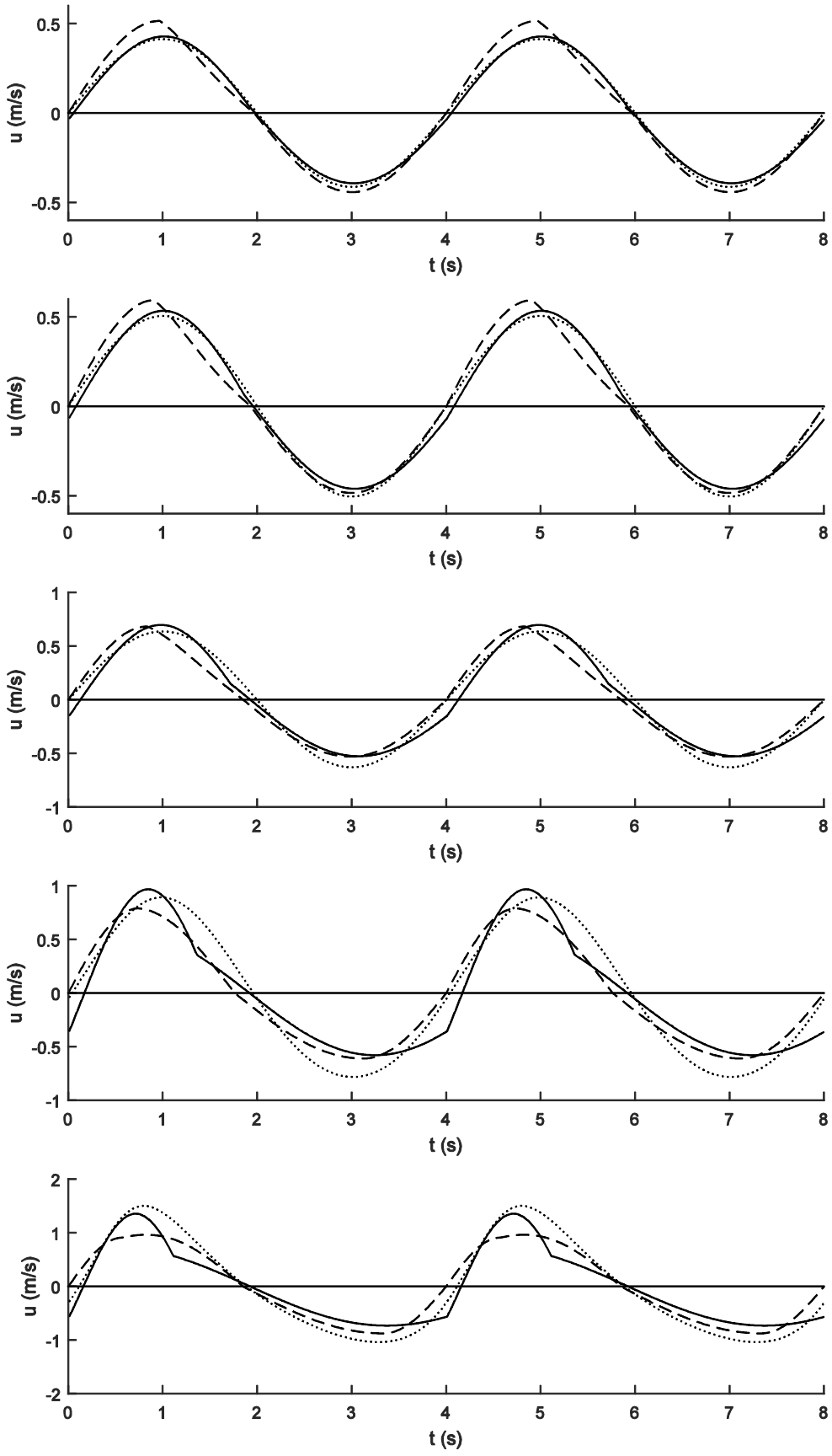

Figure 2.10: *H*=0.75m, *T*=4s, from top to bottom *h*=3.75, 3, 2.25, 1.5, 0.75m, solid line: Isobe & Horikawa (1982), dashed lines Elfrink *et al.* (2006) and dotted lines Ruessink *et al.* (2012)

Again Isobe & Horikawa (1982) and Ruessink *et al.* (2012) are most sensitive to the applied changes, but this time it is the *h*. The velocity maxima and minima, skewness and asymmetry all change more with those two parameterisations than with Elfrink *et al.* (2006), which is more constant. Ruessink *et al.* (2012) is a sine shape from *h*=2.25m to *h*=3.75m.

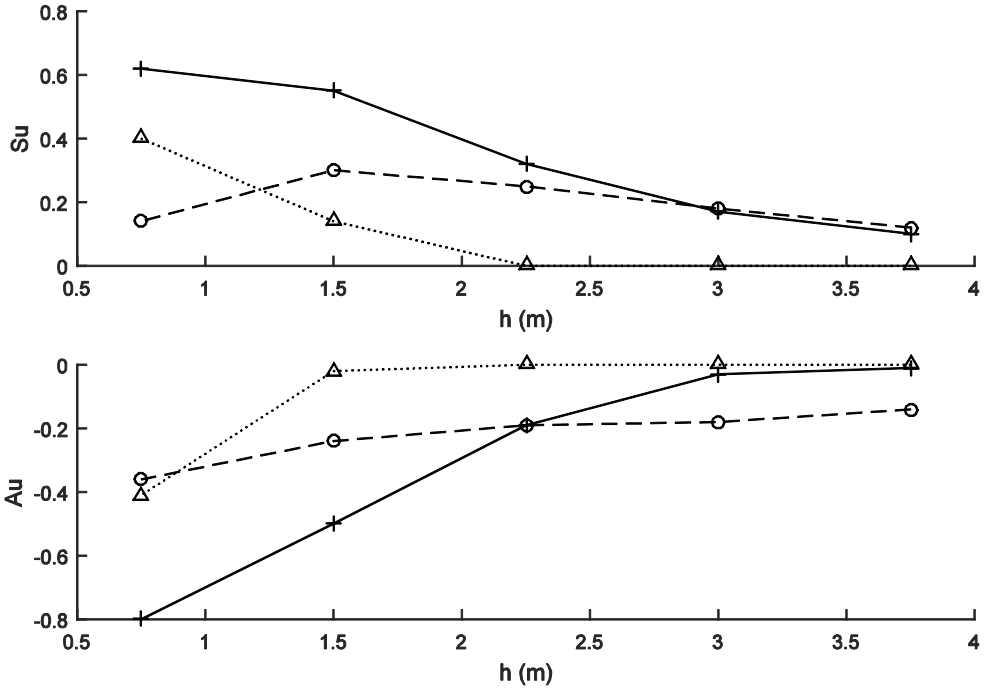

Figure 2.11: Top figure: S_u over h, bottom figure: A_u over h, plus (solid line): Isobe & Horikawa (1982), circle (dashed line): Elfrink *et al.* (2006), triangle (dotted line): Ruessink *et al.* (2012)

Table 2.2: Values of skewness and asymmetry depicted in Figure 2.11

	Isobe & Horikawa (1982)					Elfrink *et al.* (2006)					Ruessink *et al.* (2012)				
h (m)	3.75	3.0	2.25	1.5	0.75	3.75	3.0	2.25	1.5	0.75	3.75	3.0	2.25	1.5	0.75
Su	0.10	0.17	0.32	0.55	0.62	0.12	0.18	0.25	0.30	0.14	0.00	0.00	0.00	0.14	0.40
Au	-0.01	-0.03	-0.19	-0.50	-0.80	-0.14	-0.18	-0.19	-0.24	-0.36	0.00	0.00	0.00	-0.02	-0.41

The figure support the remarks made above, Elfrink *et al.* (2006) is a lot more constant than the other two. The values of skewness and asymmetry for Ruessink *et al.* (2012) are zero, between *h*=2.25 and *h*=3.75. Ruessink *et al.* (2012) becomes sinusoidal a lot earlier than the other two parameterisations.

Figure 2.12 shows the parameterisations for different values of *H*, *h* and *T* remain constant.

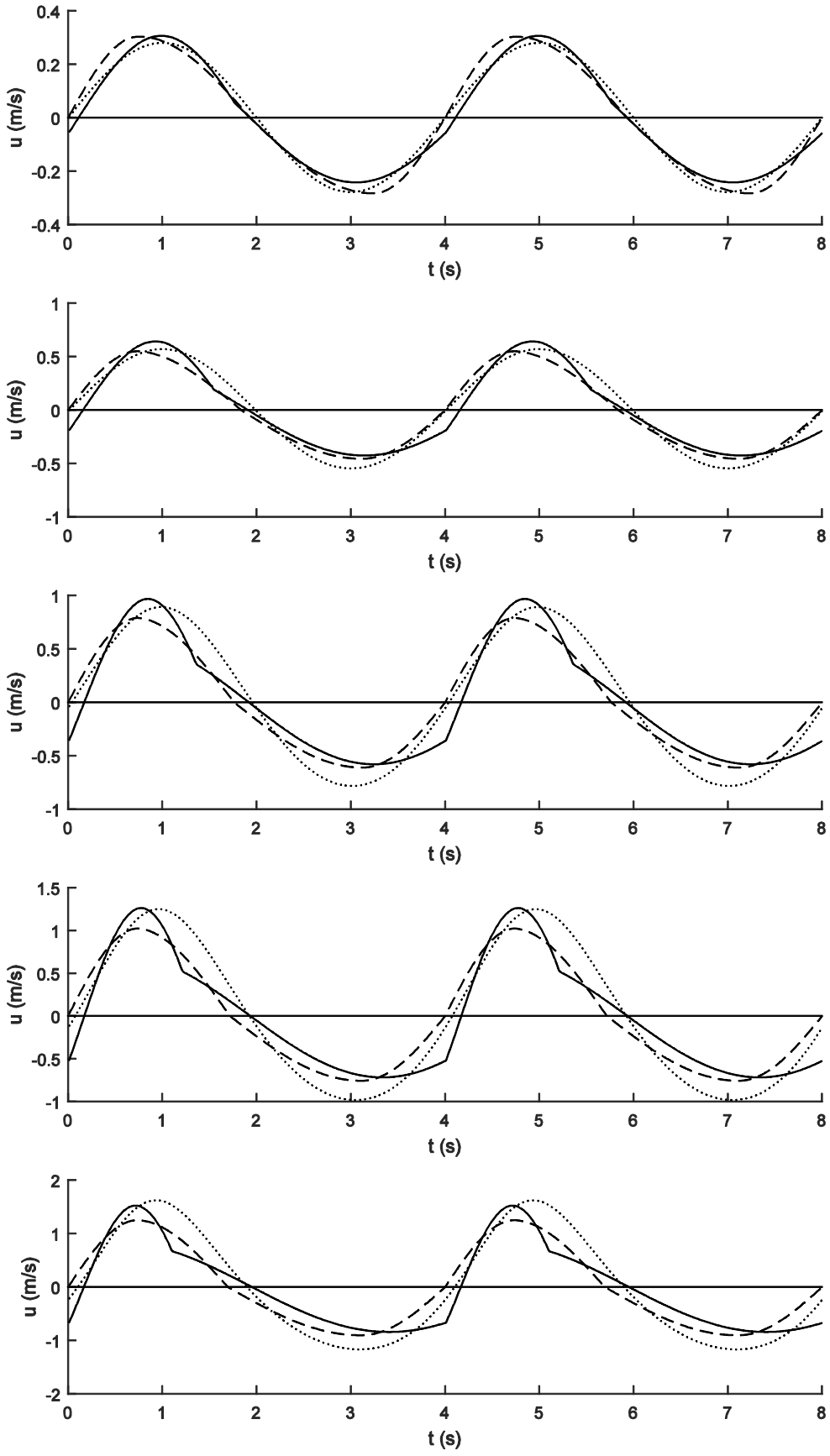

Figure 2.12: *h*=1.5m, *T*=4s, from top to bottom *H*=0.25, 0.5, 0.75, 1, 1.25m, solid line: Isobe & Horikawa (1982), dashed line: Elfrink *et al.* (2006) and dotted line: Ruessink *et al.* (2012)

All three parameterisations show a linear relationship between the wave height and the free-stream velocity. Elfrink *et al.* (2006) is only slightly less sensitive for the maxima and minima.

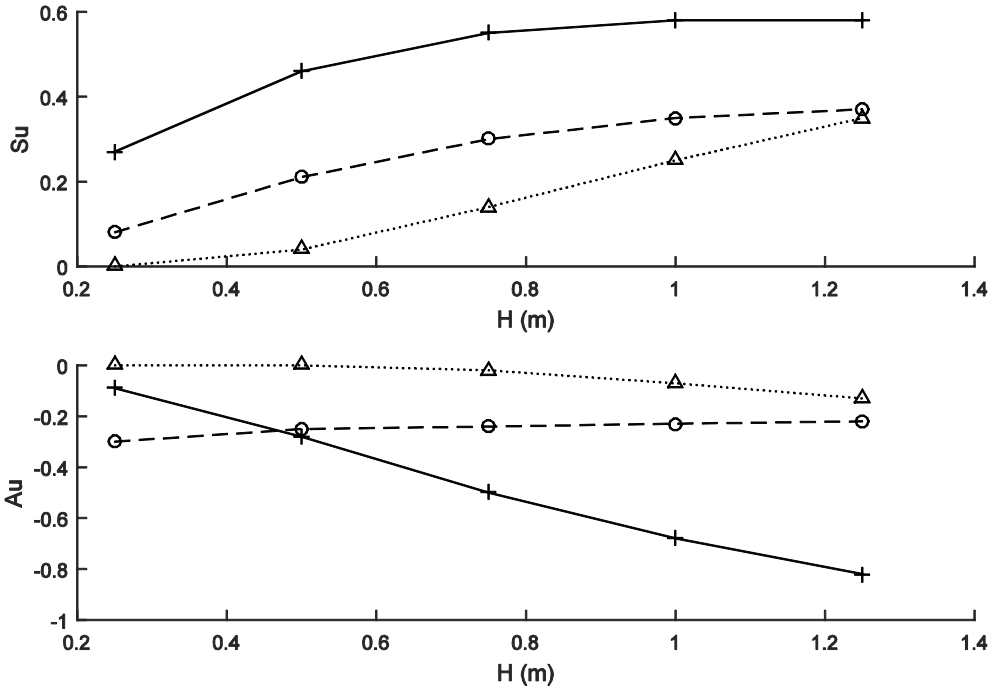

Figure 2.13: Top figure: S_u over H, bottom figure: A_u over H, plus (solid line): Isobe & Horikawa (1982), circle (dashed line): Elfrink *et al.* (2006), triangle (dotted line): Ruessink *et al.* (2012)

Table 2.3: Values of skewness and asymmetry depicted in Figure 2.13

	Isobe & Horikawa (1982)					Elfrink *et al.* (2006)					Ruessink *et al.* (2012)				
H (m)	0.25	0.50	0.75	1.0	1.25	0.25	0.50	0.75	1.0	1.25	0.25	0.50	0.75	1.0	1.25
Su	0.27	0.46	0.55	0.58	0.58	0.08	0.21	0.30	0.35	0.37	0.00	0.04	0.14	0.25	0.35
Au	-0.09	-0.28	-0.50	-0.68	-0.82	-0.30	-0.25	-0.24	-0.23	-0.22	0.00	0.00	-0.02	-0.07	-0.13

Elfrink *et al.* (2006) is very constant for the asymmetry, showing much less change than Isobe & Horikawa (1982). Ruessink *et al.* (2012) has very little asymmetry for most values of *H,* it does show some skewness from *H*=0.75m to *H*=1.25m. Isobe & Horikawa (1982) is again most sensitive and show most skewness and asymmetry.

Ruessink *et al.* (2012) only starts showing skewness and asymmetry at low values of *h* and high values of *H*, for the differing values of *T* it showed more skewness and asymmetry. Elfrink *et al.* (2006) remains very constant under the changes that were made in the input. Isobe & Horikawa (1982) shows most response to the changes and also has a lot of skewness and asymmetry.

3. Experiments

In 2014, between September and November, tests were conducted as part of the SINBAD project. The experiments were performed by Dominic van der A., Joep van der Zanden, Quim Sospedra and Iván Cáceres. Its objective was: "To obtain detailed measurements of the bottom boundary layer and outer layer hydrodynamics and bed shear stresses under large-scale breaking wave conditions (Van der A & Cáceres, 2015)."

3.1. Test facility

The experiments were conducted in Barcelona, at the Universitat Politècnica de Catalunya (UPC). There is a large wave flume; the Canal d'Invesitgació I Experimentació Mariítima (CIEMLAB), it is 100m long, 3m wide and 4.5m deep.

3.2. Test conditions

Three experiments were carried out, two mobile bed experiments and one fixed bed experiment. The data from the fixed bed experiment is used in this thesis. The fixed bed was constructed as follows: A sand bed was prepared in the flume, which had a section with a 1:10 slope followed by a horizontal section of 1.25m in height. The horizontal section is followed by a fixed parabolic shaped beach, with an average slope of 1:15. After the bed was shaped by waves of T=4s and H=0.85m during an hour, 0.1m of sand was removed from the whole length of the bed and concrete was poured to replace this. After the curing process, effort was put into making the bed as smooth as possible and rough parts where plastered with cement. The steepest part of the profile became the roughest, because some of the smoother concrete had seeped away leaving the rougher part of the mixture behind. The final roughness of the bed varied between 2-5mm.

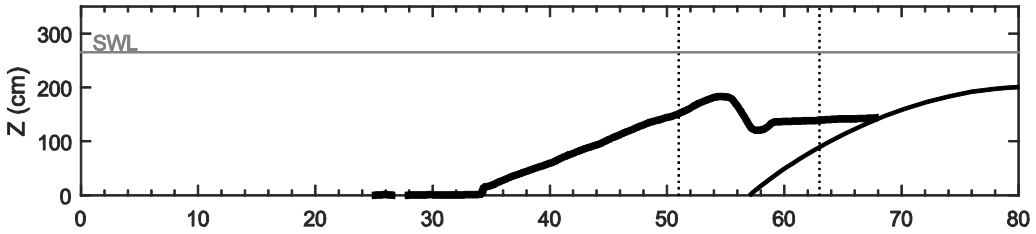

Figure 3.1: Test bed, at 0m the wave paddle is located, between the dotted line (51m-63m) the relevant tests for this thesis were carried out

The experiments were conducted with regular waves of T=4s and H=0.85m at the wave paddle.

3.3. Measurements

A wide range of measurements were made during the experiments. Here we focus only on the measurements of water surface elevation and the measurements of water particle velocities above the wave boundary layer. The following instruments were used in the measurements:

- **Acoustic Doppler Velocimeter (ADV)**
  The ADV uses the Doppler effect to measure the water velocity. To do so it must be inserted in the water flow. It measures the water velocity with ±0.5% accuracy. At 12 locations the free-stream velocity was measured closest to the bed, between 0.33m and 0.43m above the bed (see Figure 3.2). These points will be used in the data analysis.

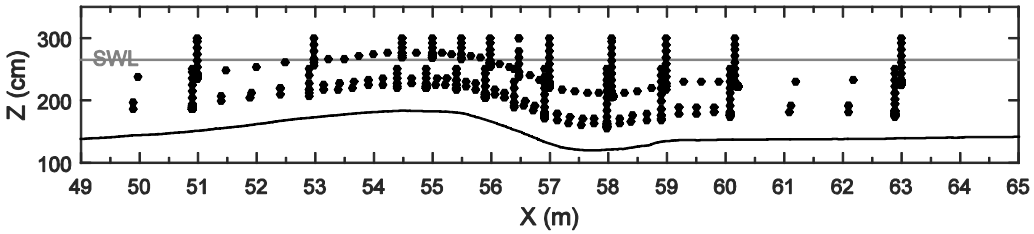

Figure 3.2: Locations where the ADV was used to measure velocities (the horizontal shoreward direction is used in this thesis)

- **Resistance Wave Gauges**
  The wave height is measured by measuring the resistance in a partially submerged electrical circuit. From the electrical current running through the device, the wave height can be measured. It allows the measurement of wave heights up to 2m. RWGs measured the wave height at several locations, as shown in Figure 3.3. The measurement at *x*=10m will be used as input for Isobe & Horikawa (1982).

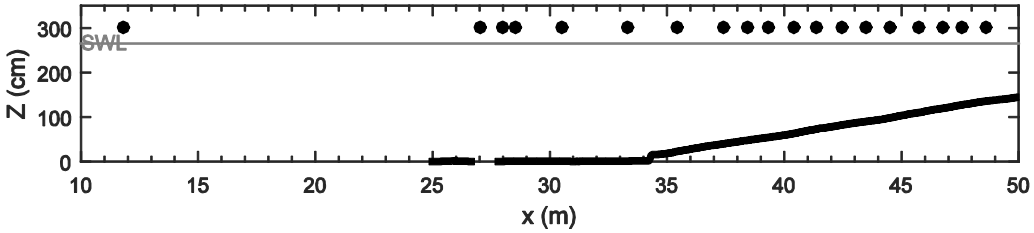

Figure 3.3: Locations at which the RWG was used to measure the wave height

- **Pore Pressure Sensors (PPT)**
  Pressure sensors were also used to measure the wave height. On some positions, data from the RWG overlaps the data from the PPT, which gave the researchers an opportunity to check the accuracy. The twelve points of measurement, which where closest to the measurement locations of the ADV are selected for input into the parameterisations. The PPT measurements that are used, come from the PPTs attached to the mobile frame pictured in Figure 3.6.

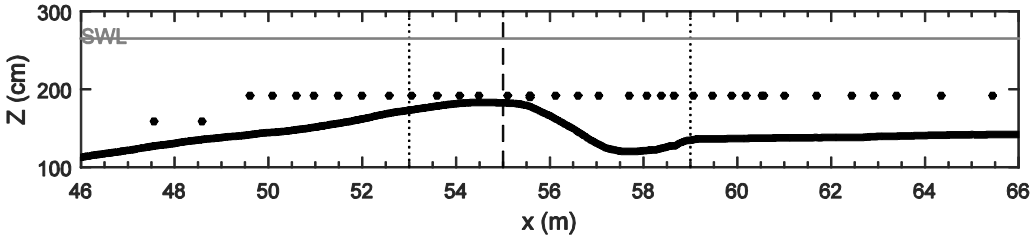

Figure 3.4: Locations where PPT's were used to measure the wave height

Figure 3.5: Upper left: Acoustic Doppler Velocimeter. Retrieved from: SonTek, upper right: Resistive Wave Gauge. Source: Van der A & Cáceres (2015), Bottom: Pore Pressure Sensors. Retrieved from: Van der A & Cáceres (2015)

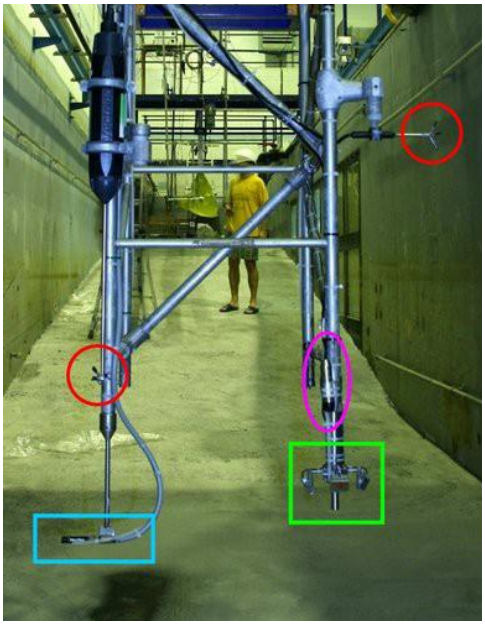

Figure 3.6: Mobile frame, Red: ADV's, Green: ADVP, Blue: LDA and Pink: PPT. Retrieved from: Van der A & Cáceres (2015)

3.4. Measured free-stream velocities

The free-stream velocities that were measured are driven by the time-ranging free surface elevation. Five locations are shown here to show this connection at different points in the breaking process and see if they match expectations.

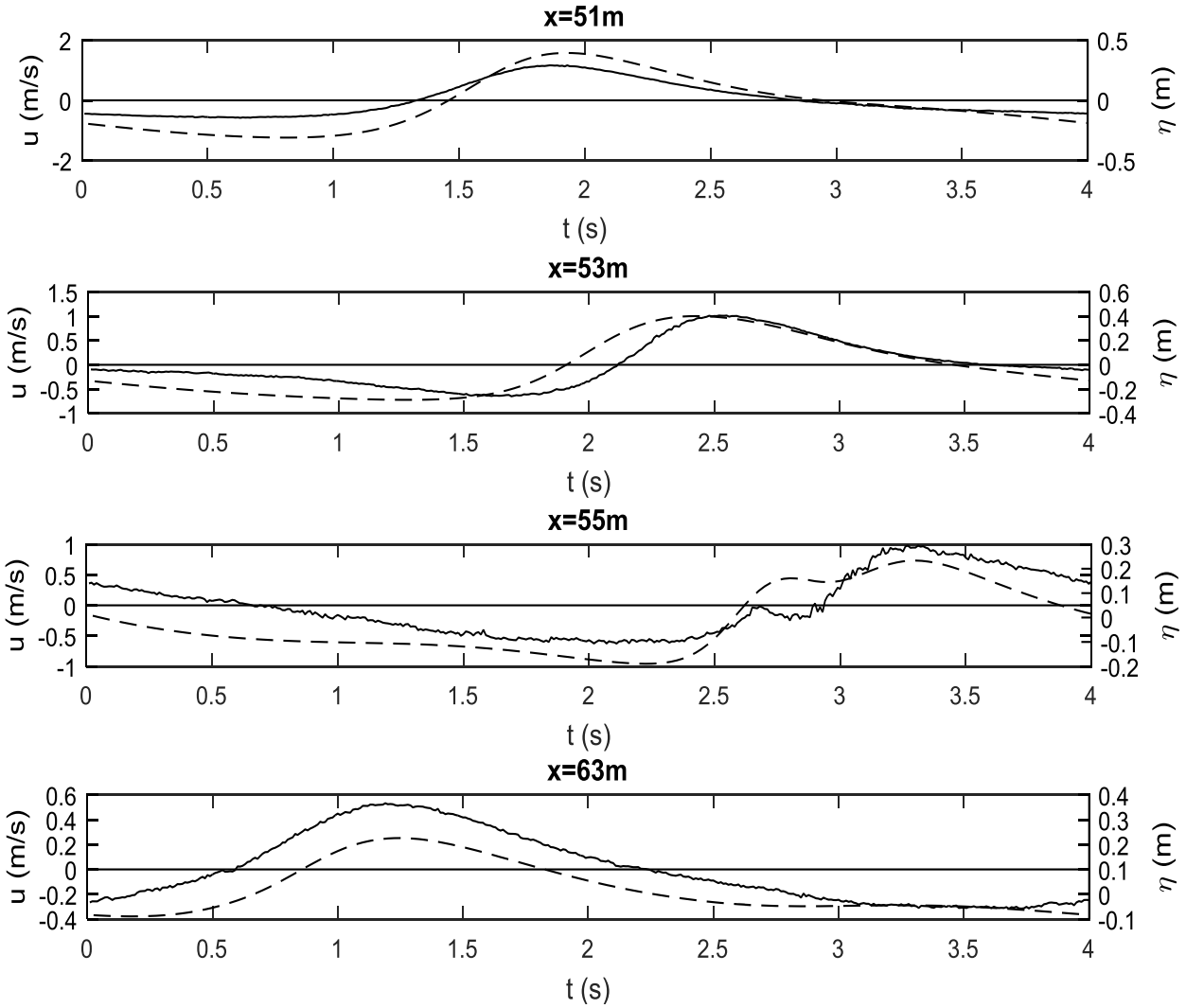

Figure 3.7: Solid line: free-stream velocity (u_0), dashed line: free-surface elevation (H) at: from top to bottom 51m, 53m, 55m and 63m

At 51m (Figure 3.7) the wave has not yet begun breaking, the connection between the measured velocity and measured surface elevation is clearly visible here. The top of the crest matches with the highest free-stream velocities and the trough has the highest negative free-stream velocities.

At 53m the wave begins the breaking process, as seen by van der A. (personal communication, June, 2015). It is shown that the connection between free-stream velocity and the water surface elevation is now a little different. The most notable difference is that free-stream velocity remains negative for a while even though the crest of the wave passes by.

At 55m the wave breaks, according to van der A. (personal communication, June, 2015). Again the water-particle velocity stays negative while the water surface elevation has already risen strongly. The water particle velocity also shows small fluctuations which are not present in the free-surface

elevation; these fluctuations might be noise related to breaking-induced air reaching the velocity measurement point.

Further onshore, at 63m, the relation between the free-stream velocity and free surface elevation is again as seen at 51m.

The expectations regarding the free-stream velocity between the shoaling and surf zone are: At first the maximum and minimum velocities increase with the increasing wave height until breaking. After the breaking point the decreasing wave height also leads to a decrease in maximum and minimum velocities. The skewness increases until the wave reaches its maximum skewness at the breaking point, after which the skewness will decrease along with the decreased wave height. The asymmetry will increase up to the breaking point, after which it will remain high or will even increase as the wave bore has a high asymmetry.

3.5. Methodology

To obtain the free-stream velocities shown above the averaged data obtained from the experiments was first smoothened, using the 'smooth' function in Matlab. It was decided to smooth the free-stream velocity time series to prevent irregularities determining the peak velocities. The undertow (the near-bottom current in offshore direction) was also removed from the measured data by applying detrend in Matlab. Appendix C shows the smoothened versus the non-smoothened time series, Appendix D shows the data before and after removing the undertow.

Because the velocities were measured at between 0.33m and 0.43m above the bed the measured velocities have been translated using linear wave theory (Equation 3.1) to 0.2m above the bed, so that they can be compared more accurately with the parameterisations.

$$u_{new} = u - u\left(\frac{\cosh\big(k(y+h)\big)}{\sinh(kh)} - \frac{\cosh\big(k(0.2+h)\big)}{\sinh(kh)}\right) \tag{3.1}$$

where *y* is the height above the bed at which the velocity was measured. The translated velocities are on average 11.6% lower than before the translation. Figure 3.8 is an example to show the change in orbital velocities.

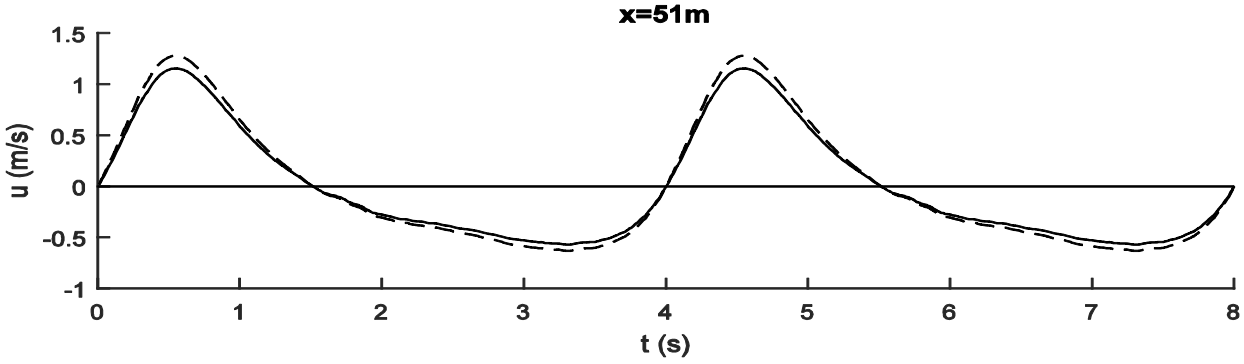

Figure 3.8: Example of the translation, at x=51m, dashed line: measured velocity, solid line: new velocity

The equations of the parameterisations and the equations for calculating the skewness and asymmetry parameters were scripted in Matlab with the parameters as input.

3.6. Measured parameters

The relevant measured parameters for the parameterisations are shown in

Table 3.1. These values are used as input for the parameterisations to compute the free-stream velocity.

Table 3.1: Measured parameters

Location (m)	Water depth (m)	Wave height (m)	Bed slope	Offshore wave height (m)
51	1.14	0.70	0.1	0.66
53	0.96	0.69		
54.5	0.82	0.43		
55	0.83	0.42		
55.5	0.87	0.36		
56	1.03	0.36		
56.5	1.19	0.39		
57	1.35	0.38		
58	1.43	0.35		
59	1.30	0.35		
60	1.28	0.36		
63	1.26	0.32		

The water depth reduces as the measurement location approaches the bar, afterwards the water depth rises as the trough is entered. At the end of the trough the water depth becomes shallower again, first quickly and behind the trough very slowly. Throughout all of the measurement locations the wave height shows a steady decline. The bed slope is measured only once, as the average bed slope over a longer distance is required for the parameterisations that use it.

4. Data Analysis and Discussion

In this chapter, the measured data and the results will be discussed and a comparison between them will be made. The comparison begins by first presenting the measured and parameterised velocity time-series for each of the 12 cross-shore locations. After that the maximum velocities, skewness and asymmetry are shown and discussed. For further information the acceleration time series can be found in Appendix D.

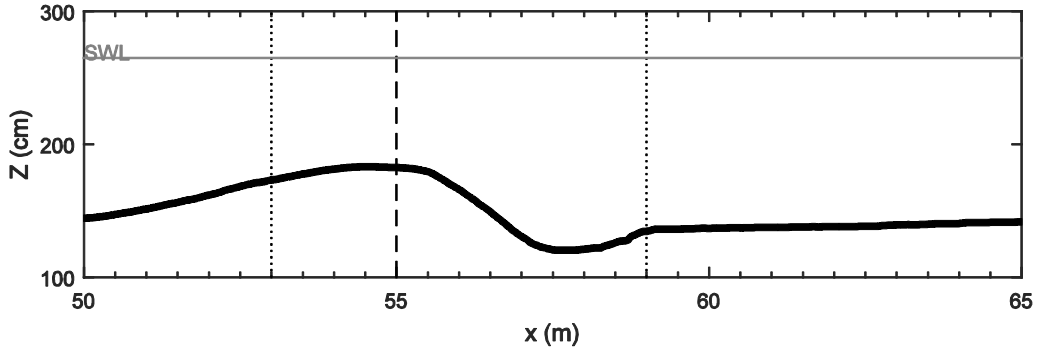

Figure 4.1: The measurement location, dotted lines mark the breaking zone and the dashed line markes the breaking point as seen by van der A. (personal communication, June, 2015)

Figure 4.1 shows the bed over the length of the measurements and the breaking zone and breaking point, as reference for the data.

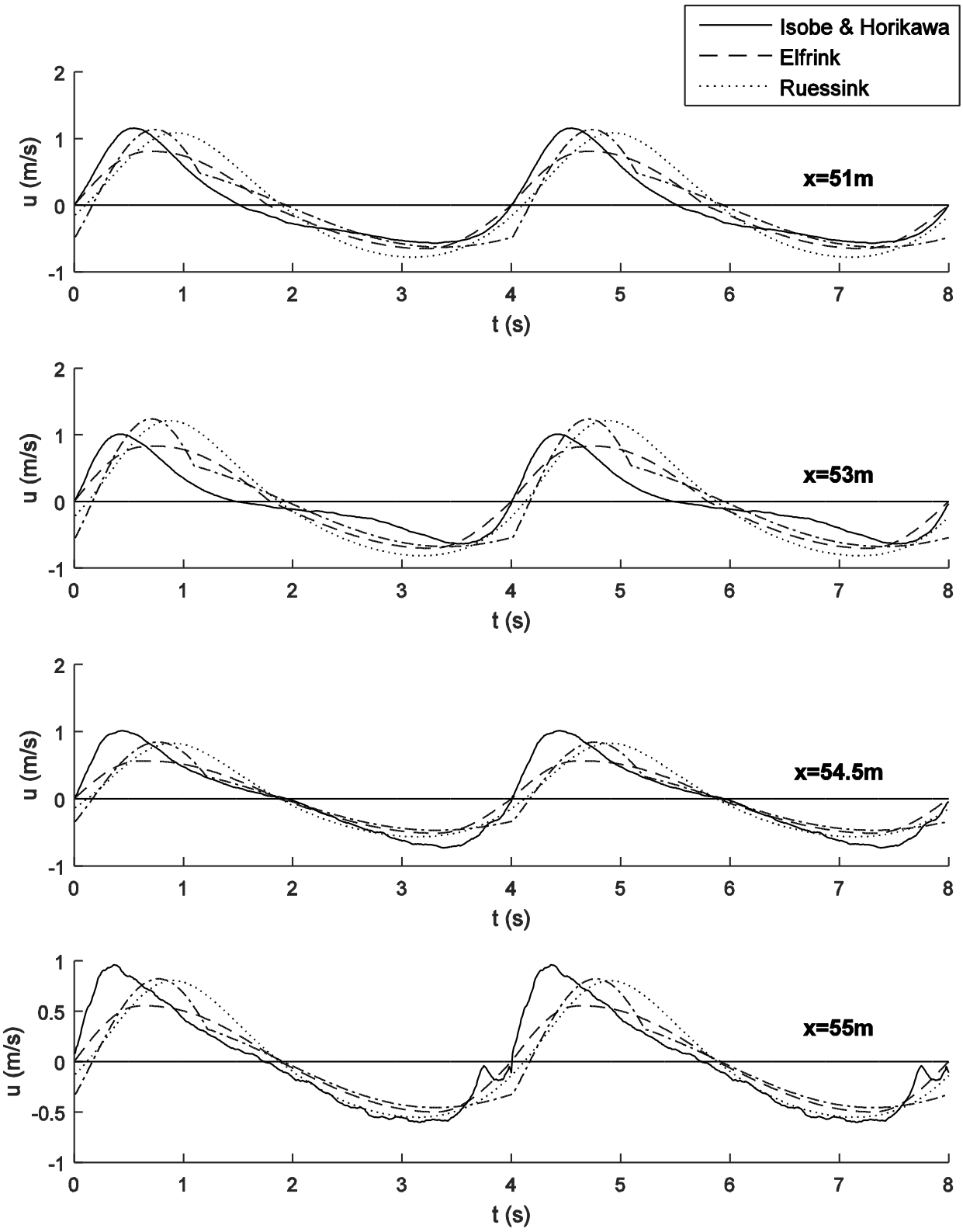

Figure 4.2 Measured and computed free-stream velocity time series for four locations between 51m and 55m (pre-breaking to breaking), solid line: measured velocities, dash-dotted: Isobe & Horikawa (1982), dashed line: Elfrink *et al.* (2006), dotted line: Ruessink *et al.* (2012)

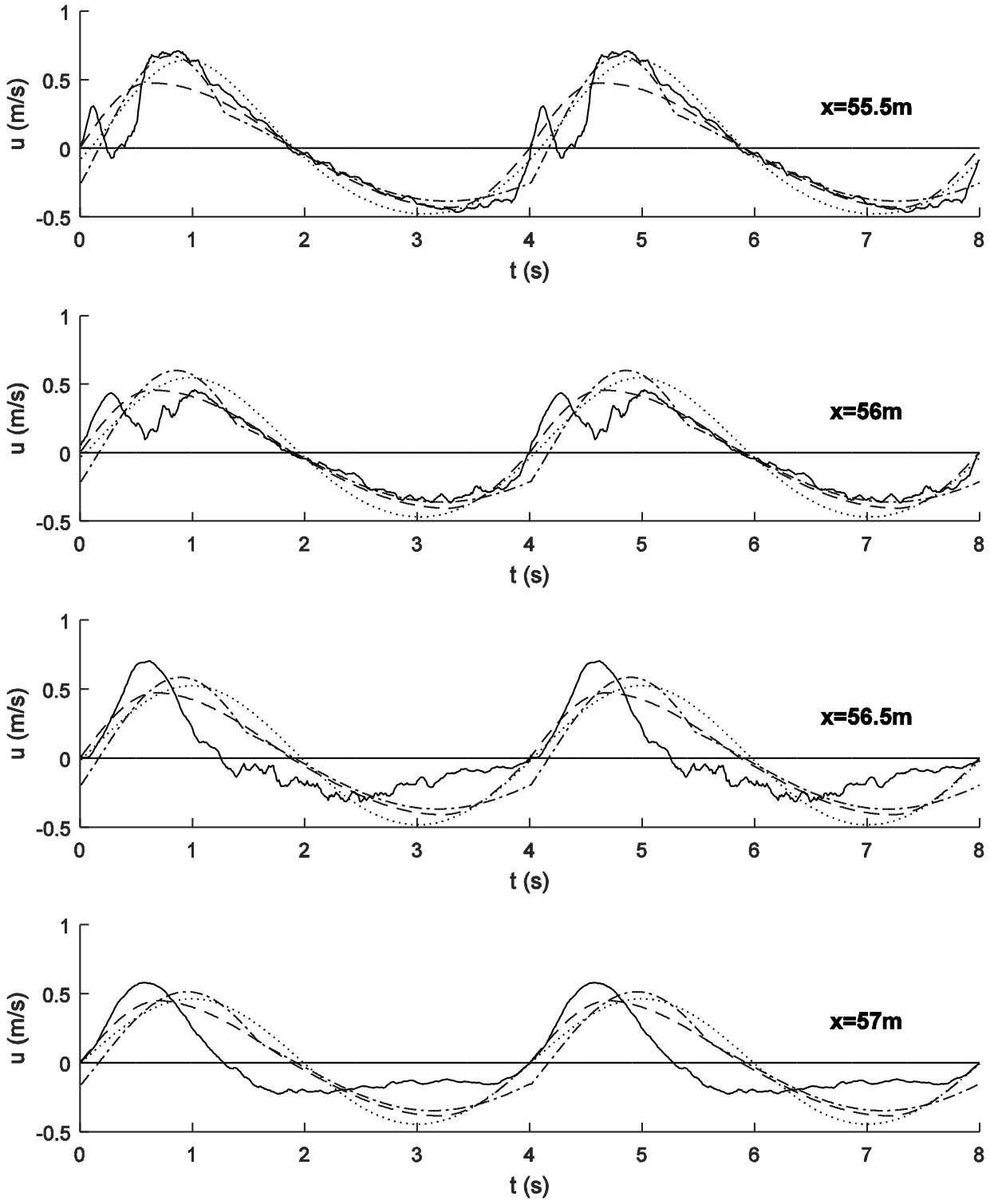

Figure 4.3: Measured and computed free-stream velocity time series for four locations between 55.5m and 57m (after breaking), solid line: measured velocities, dash-dotted: Isobe & Horikawa (1982), dashed line: Elfrink *et al.* (2006), dotted line: Ruessink *et al.* (2012)

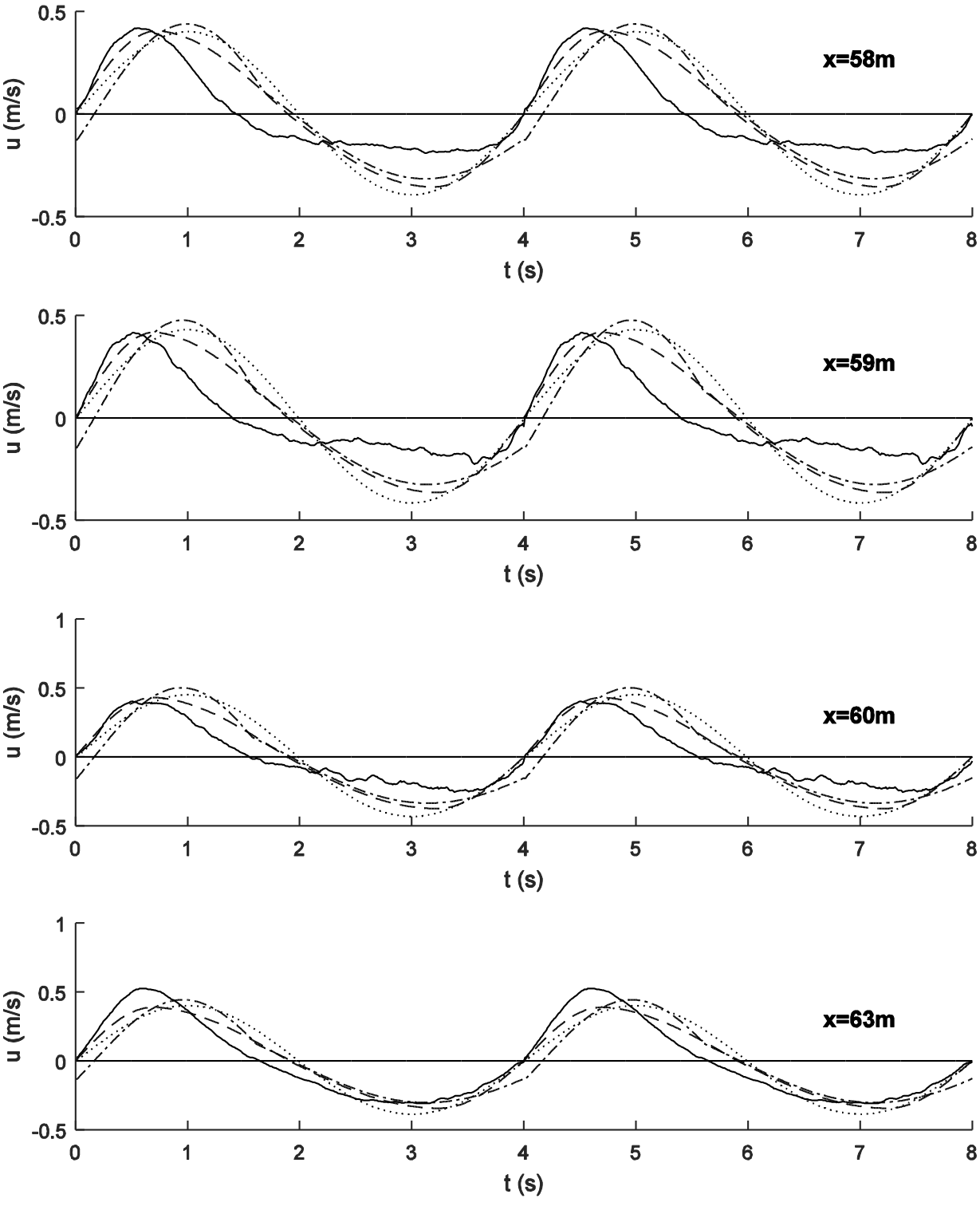

Figure 4.4: Measured and computed free-stream velocity time series for four locations between 58m and 63m (after breaking to uniform bore), solid line: measured velocities, dash-dotted: Isobe & Horikawa (1982), dashed line: Elfrink *et al.* (2006), dotted line: Ruessink *et al.* (2012)

Figure 4.2, Figure 4.3 and Figure 4.4 show the measured and parameterised velocity time-series for x=(51,53,54.5 and 55m), x=(55.5,56,56.5 and 57m) and x=(58,59,60 and 63m), respectively. Note that results in Figure 4.2 correspond to the pre-break/break positions, while the results in Figure 4.3 correspond to the after breaking positions and Figure 4.4 to after breaking and uniform bore positions. It is difficult to compare the measured and parameterised time-series directly. Instead we compare single-value measures of the primary characteristics (maximum and minimum velocity, and skewness and asymmetry) in the following.

4.1. Maximum and minimum velocity

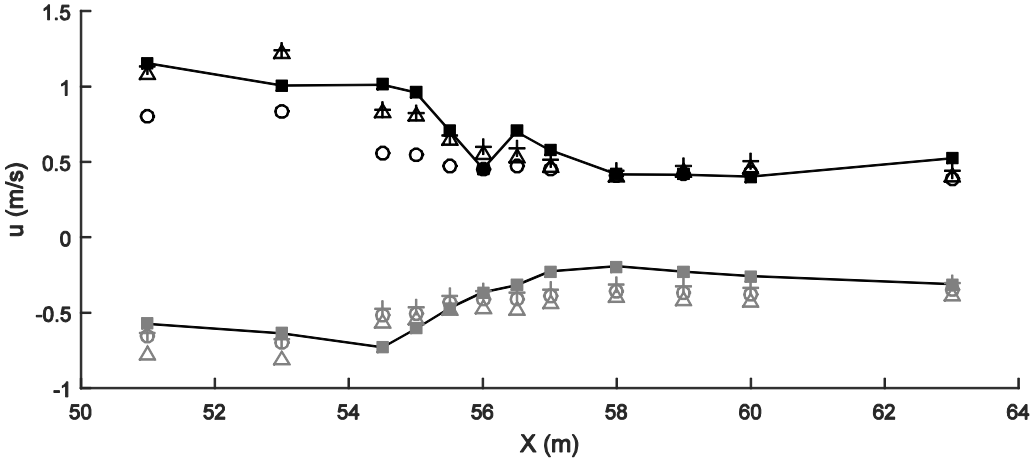

Figure 4.5: Maximum (black) and minimum (grey) free-stream velocity, square: measured, plus: Isobe & Horikawa (1982), circle: Elfrink *et al.* (2006), triangle: Ruessink *et al.* (2012)

Figure 4.5 presents the maximum and minimum velocities from the measured and parameterised velocity time-series presented in Figure 4.2-Figure 4.4. The measured maximum velocity shows a small decrease at the start. In the breaking zone there is a sharp decrease in maximum velocity and nearing the end it becomes fairly constant and increases slightly after the breaking zone. At 53m the maximum water particle velocity is lower than would be expected when we look at the trend of the graph. This may be due to the start of the wave breaking process here. At 55.5m and 56m there is a far smaller maximum velocity than at the locations immediately next to them, this could be due to the breaking of the wave at 55m and the irregular wave behaviour accompanying that. It can however also be a measurement error, caused by air bubbles which are not uncommon in that region and can affect the measurements. The measured maximum velocities don't show very strange values or value changes and mostly behave as expected.

Ruessink *et al.* (2012) and Isobe and Horikawa (1982) show reasonably good agreement in terms of maximum velocity. The trend is depicted reasonably well over the entire length of the measurements. *x*=53m is interesting because the two parameterisations predict a rise in the velocity, while the measured velocities decrease. Figure 4.3 shows that at 56m, 56.5m and 57m the measured maximum velocity decreases, increases and decreases again, something the parameterisations are unable to show. When we look at the measured velocity time series at 56m there is a clear collapse in free-stream velocity where the velocity time series otherwise would have reached its maximum. This could be due to irregularities of the flow in the breaking zone that are not represented in the parameterisations, but it can also be the result of air bubbles affecting the measurements.

The maximum velocity estimation of Elfrink *et al.* (2006) is too low for most cases and too constant. This is something that was seen in the intercomparison as well, chapter 2.4. There is a clear underestimation of the velocity in the region 51m-55m. In the region from 58m and onwards Elfrink *et al.* (2006) estimates the velocity better, coming close to the measured results. This is however only the result of not showing the right trend; where the measured data shows a decrease this parameterisation remains constant.

The measured minimum velocity increases up till 54.5m, after which it starts to decrease strongly until 58m. During almost the entire breaking zone the measured minimum velocity decreases. After the breaking zone, the measured minimum velocity increases a little again. The measured minimum velocity behaves as expected, the decrease is a logical result of the loss of energy during the breaking process.

All three parameterisations show the same trend for the minimum velocity. It is similar to the trend of the measured velocities but, the decrease in minimum velocity is smaller and happens over a longer time span. The parameterisations have significant margins of error for the minimum velocities, the estimations is at some points more than 50% off. The minimum velocities are mostly overestimated, but for 54.5m-55.5m they are underestimated.

4.2. Skewness

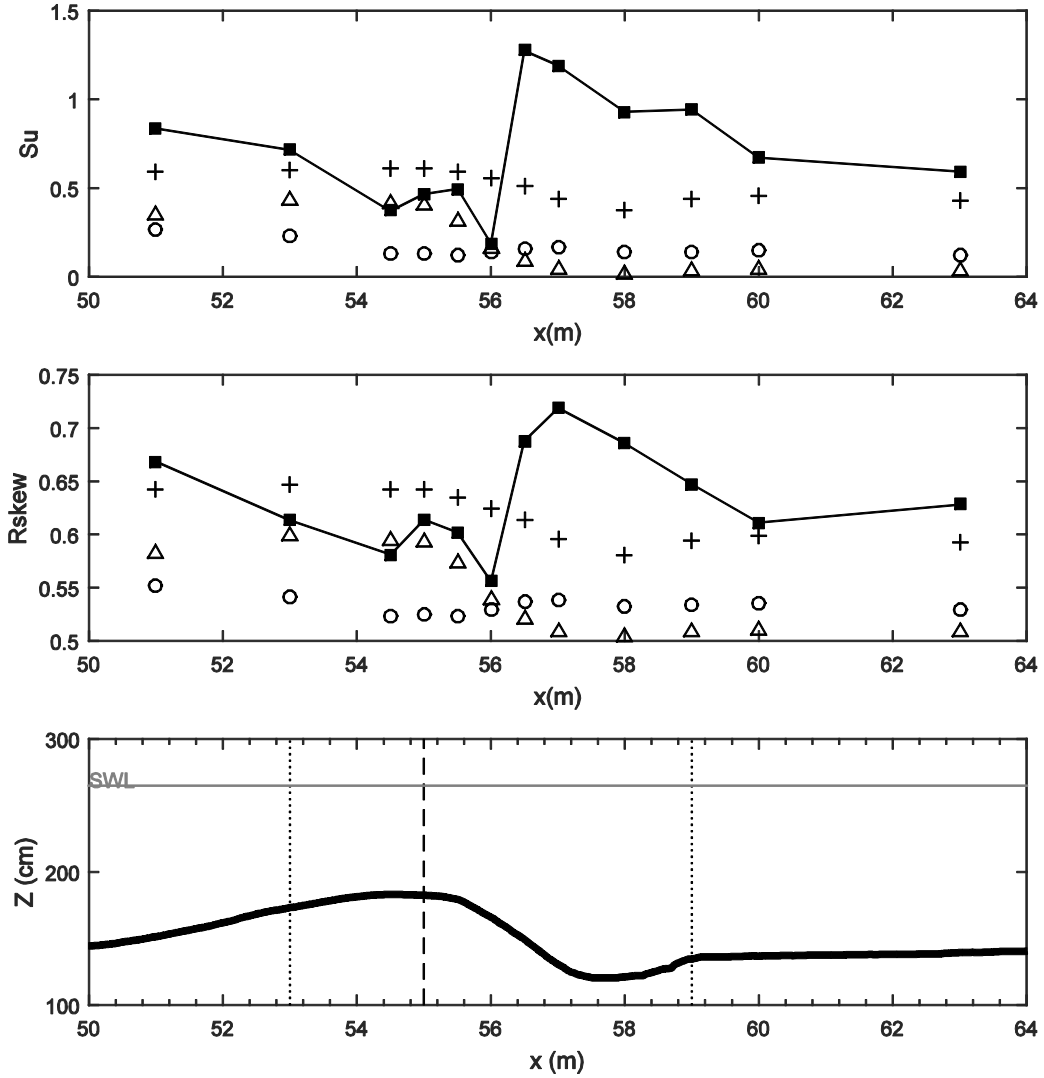

Figure 4.6: Top figure: S_u (skewness) at the locations, middle figure: R_{skew} at the locations, square: measured, plus: Isobe & Horikawa (1982), circle: Elfrink *et al.* (2006), triangle: Ruessink *et al.* (2012), the bottom figure shows the bed of the wave flume

Figure 4.6 presents the skewness (S_u) from the measured and parameterised velocity time-series presented in Figure 4.2-Figure 4.4. The measured skewness shows a decrease between 53m-56m where an increase might be expected as the waves become more nonlinear on the approach to breaking. When we look at the measured velocity time series Figure 4.3, we see that especially at 55.5m and 56m the maximum velocity is decreased. This was noted earlier already, these results could be influenced by measurement errors due to air bubbles. The velocity time series seem to behave as expected from 53m-55m. From 56.5m the skewness decreases slightly and thus behaves as expected.

None of the parameterisations seem to be able to capture the trend of the measured skewness. They are more or less constant and their values are generally too low. Their skewness should be decreasing slowly and then increase sharply, shortly after the breaking of the wave and then descend from 56.5m onwards. Isobe & Horikawa (1982) and Ruessink *et al.* (2012) do not show the increase after breaking but do show the decrease between 56.5m and 58m. The decrease is however too

small for Isobe & Horikawa (1982). The decrease of Ruessink *et al.* (2012) is more or less the same size as the measured data, but as it doesn't show the increase first this leads to a significant underestimation of the skewness. Skewness in the case of Elfrink *et al.* (2006) stays constant at a low value, nothing like the measured or expected results.

The middle graph in Figure 4.6 presents the skewness (R_u) from the measured and parameterised velocity time-series presented in Figure 4.2-Figure 4.4. The R_{skew}, is a different measure for the skewness, but as can be seen shows mostly the same behaviour as S_u. Different values of course, but almost exactly the same trends.

4.3. Asymmetry

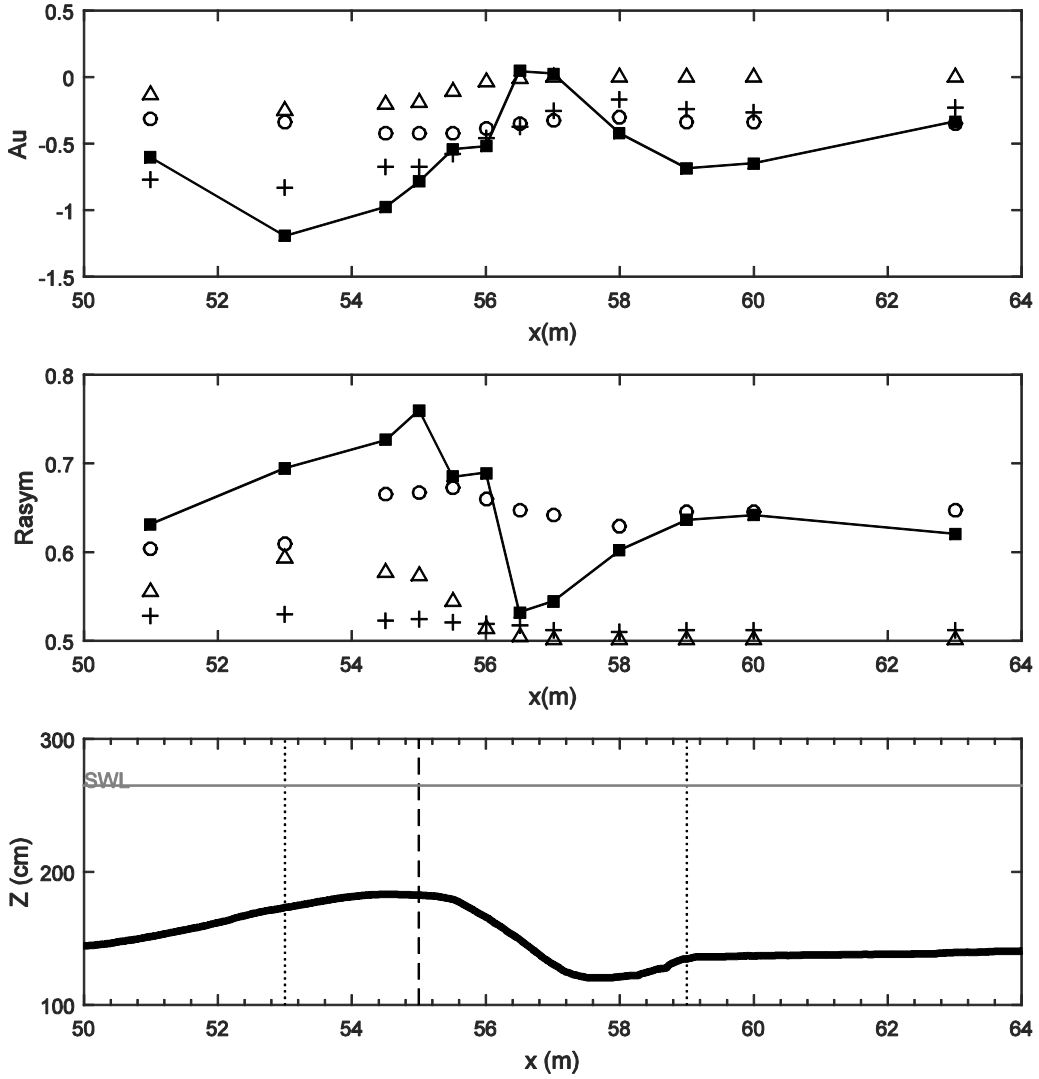

Figure 4.7: Top figure: A_u (asymmetry) at the locations, middle figure: R_{asym} at the locations (higher positive values mean higher asymmetry, mirror of A_u), square: measured, plus: Isobe & Horikawa (1982), circle: Elfrink *et al.* (2006), triangle: Ruessink *et al.* (2012). Further negative is higher asymmetry, the bottom figure shows the bed of the wave flume

The top graph in Figure 4.7 presents the asymmetry (A_u) from the measured and parameterised velocity time-series presented in Figure 4.2-Figure 4.4. The measured A_u shows an increase in asymmetry until the breaking of the wave starts, at x=53m, and a rapid decrease in A_u thereafter. It was expected that A_u would stay more constant in and after the breaking zone. After breaking the

wave bore shows a fairly constant asymmetry, in line with expectations. At, x=56m and x=56.5m, the measured asymmetry is very low. This is unexpected and it could be that local influences are affecting the measurements, leading to the decrease in asymmetry.

From the top graph in Figure 4.7 it is clear that Elfrink *et al.* (2006) and Ruessink *et al.* (2012) heavily underestimate the asymmetry. Ruessink *et al.* (2012) shows a small decrease where the measured data also decreases, up to 57m it seems to follow the trend of the measured velocity only being far too small and the trend far too subtle. Because the trend at least seems to be there, Ruessink *et al.* (2012) might perform better when calibrated specifically for this situation. Elfrink *et al.* (2006) shows little change over the different locations, again being very constant. Isobe & Horikawa (1982) shows the most similarity with the measurements in terms of trend and asymmetry values. Up to 56m the trend is similar to the measured trend. The line between 53m and 56m is less steep than the measured data, but it comes close. After 57m Isobe & Horikawa (1982) stays mostly constant, where the measured data shows a significant increase in asymmetry.

The middle graph in Figure 4.7 presents the asymmetry (R_{asym}) from the measured and parameterised velocity time-series presented in Figure 4.2-Figure 4.4. Interestingly the R_{asym} shows mostly the same trends, except Isobe & Horikawa (1982). The figure is a mirror of Figure 4.7 for most locations. Isobe & Horikawa (1982) however is very constant and very low over the entire length. R_{asym} is calculated from the maximum and minimum acceleration, therefore we will look at the acceleration time series to better understand the behaviour.

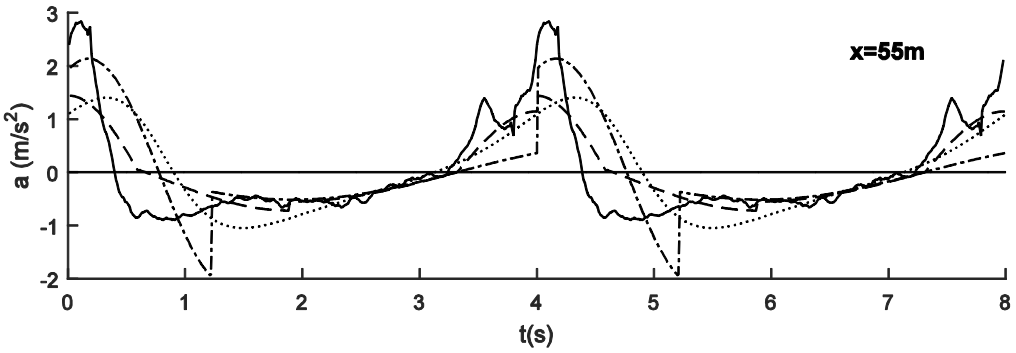

Figure 4.8: Acceleration time series at x=55m, solid line: measured acceleration, dash-dotted: Isobe & Horikawa (1982), dashed line: Elfrink *et al.* (2006), dotted line: Ruessink *et al.* (2012)

Figure 4.8 presents the acceleration time series derived from the measured and parameterised velocity time-series presented in Figure 4.2-Figure 4.4. The discontinuity of the velocity time series of Isobe & Horikawa (1982) causes very large and short negative acceleration peaks, which can be seen in Figure 4.8. This leads to values for the R_{asym} which are different from the A_u. For depicting the measured data and Isobe & Horikawa (1982) the R_{asym} is therefore not very good, as it only looks at the maximum and minimum instead of the entire time-series like A_u. Figure 4.8 is only one example of the acceleration time series, the others can be found in Appendix D and support the findings here.

5. Conclusions and Recommendations

This thesis set out to answer the following question: How well do free-stream velocities estimated using the parameterisations of Isobe & Horikawa (1982), Elfrink *et al.* (2006) and Ruessink *et al.* (2012) compare to the measured velocities as regular waves propagate up a slope, break on a breaker bar and propagate? The study has used data from the SINBAD experiments in Barcelona to answer this question. To answer the main question, the sub questions will first be answered.

- How do the free-stream velocities estimated using the parameterisations of Isobe & Horikawa (1982), Elfrink et al. (2006) and Ruessink et al. (2012) compare to each other as regular waves propagate up a slope, break on a breaker bar and propagate?
  Elfrink *et al.* (2006) is the least sensitive to changes made in the *T, h* and *H.* Ruessink *et al.* (2012) is sinusoidal for a much longer time than the other two parameterisations, but will show skewness and asymmetry above a certain threshold. The output of Isobe & Horikawa (1982) changes most with the changes in input of the three parameterisations; it is sensitive to the changes and becomes skewed and asymmetric quicker than Ruessink *et al.* (2012).
- Does the measured data behave as expected by theory on wave breaking and does it behave realistically?
  Except for a dip in the maximum velocities at 55.5m and 56m, the measured maximum velocities show results which are to be expected. The measured minimum velocity data behaves as expected and looks realistic. Both the minimum and maximum velocities decrease slowly up to x=58m and then become constant. The skewness of the measured data decreases in the region 51m-56m, where an increase would be expected. The velocity time series show that there is a possible measurement error at 55.5m and 56m, the other measurements behave normally. The asymmetry decreases unexpectedly during and shortly after breaking; theoretically it would stay more constant there. Flow irregularities and measurement errors might be the cause of this, but it might be what happens in the breaking zone under these conditions.
- How well do the maximum and minimum free-stream velocities estimated using the parameterisations of Isobe & Horikawa (1982), Elfrink *et al.* (2006) and Ruessink *et al.* (2012) compare to the measured maximum and minimum velocities as regular waves propagate up a slope, break on a breaker bar and propagate?
  Isobe & Horikawa (1982) and Ruessink *et al.* (2012) estimate the maximum velocity reasonably well over the cross-shore extent of the measurements. Elfrink *et al.* (2006) predicts near-constant maximum velocities over the entire length of the calculations, which is unrealistic and does not match the data well. The parameterisations all show approximately the same trend for the minimum velocity. They show a decrease in the minimum velocity where the measured data shows it as well, but the decrease is much smaller.

  The conclusions on the maximum and minimum velocities are based solely on the analysis of the data on those values. The analysis of the skewness does not influence the conclusions on this, even though the skewness (R_{skew}) is dependent on them. Otherwise the maximum and minimum velocity are not tested independently.

- How well does the skewness of free-stream velocities estimated using the parameterisations of Isobe & Horikawa (1982), Elfrink *et al.* (2006) and Ruessink *et al.* (2012) compare to the skewness of the measured velocities as regular waves propagate up a slope, break on a breaker bar and propagate?
  Isobe & Horikawa (1982) does not show the rise seen in the measured data at around 56m. The decrease of the skewness shown by the measured data after that, is reproduced by Isobe & Horikawa (1982) but the decrease is much smaller. Isobe & Horikawa (1982) doesn't seem able to accurately estimate skewness. Ruessink *et al.* (2012) also does not show the increase seen around 56m, but the decrease in skewness afterwards is shown better than by Isobe & Horikawa. However this leads to a heavy underestimation of the skewness, because there is no initial increase. Overall the estimations are far off. Elfrink *et al.* (2006) predicts a skewness which is far too small and constant and doesn't match the measured data at all.

  As stated above the measured skewness shows some unexpected results and measurement errors are expected at x=55.5m and x=56m, but even when those points are excluded from the comparison the conclusions on the parameterisations will be the same.

- How well does the asymmetry of free-stream velocities estimated using the parameterisations of Isobe & Horikawa (1982), Elfrink *et al.* (2006) and Ruessink *et al.* (2012) compare to the asymmetry of the measured velocities as regular waves propagate up a slope, break on a breaker bar and propagate?
  Isobe & Horikawa (1982) shows some agreement with the measured data, up to 56m the trend is comparable but after that the estimates are more constant than the measurements. The estimated asymmetry of Isobe & Horikawa (1982) comes closest to the measurements but can still be more than 50% off. Ruessink *et al.* (2012) heavily underestimates the asymmetry and shows not enough variation with cross-shore distance. Elfrink *et al.* (2006) also heavily underestimates the asymmetry and is again too constant too accurately depict the measured data.

  Since the asymmetry behaves somewhat unexpected it is difficult to come to definitive conclusions on the accuracy of the parameterisations for the asymmetry.

How well do free-stream velocities estimated using the parameterisations of Isobe & Horikawa (1982), Elfrink *et al.* (2006) and Ruessink *et al.* (2012) compare to the measured velocities and to one another as regular waves propagate up a slope, break on a breaker bar and propagate?
Elfrink *et al.* (2006) shows very poor comparison with the measured data on every tested parameter. Ruessink *et al.* (2012) estimates the maximum velocities pretty well, on the other points the results are quite poor. Isobe & Horikawa (1982) estimates good maximum velocities and estimates the asymmetry reasonably. Isobe & Horikawa (1982) produces the best results of the parameterisations for these conditions and Elfrink *et al.* (2006) produces the poorest results.

The conclusions reached in this thesis are important for anyone using these parameterisations as input for a sand transport model, since the output of such a model relies on accurate velocities. It is not advised to use these parameterisations in the breaking zone, under the conditions tested in this thesis. Further development of these parameterisations will be very useful to produce more accurate descriptions of the free-stream velocity in the breaking zone. Especially practical applications would

benefit from an improved parameterisation since the exact methods are often too computationally demanding.

It must be noted, that the test performed in this thesis is a particularly challenging one, for which a parameterisation cannot be expected to perform perfectly. Elfrink *et al.* (2006) and Ruessink *et al.* (2012) both mention that they do not advise to use their parameterisations under these circumstances. Isobe & Horikawa (1982) is the only one calibrated with laboratory experiments and this could explain why it performs better than the other two.

Another finding of this thesis is that the R_{asym} can be a poor measure for the asymmetry for discontinuous parameterisations. As those parameterisations tend to have spikes in their acceleration time series which influence the R_{asym}, while those spikes are not representative for the acceleration time series as a whole.

A limitation of this study is that only one wave condition is tested. It is recommended to test the parameterisations against a broader range of breaking wave conditions. It is important to further develop parameterisations for the breaking region since large sand transport rates (and morphodynamic changes) take place in this region.

Following my results, I conclude that Isobe & Horikawa (1982) produces the best results under these circumstances. In these conditions I therefore advise to use Isobe & Horikawa (1982). Isobe & Horikawa (1982) however, still does not produce very satisfying results, thus making a new and better parameterisation an important focal point for further research.

Bibliography

- Abbot, M.B. & Price, W.A. (1994). *Coastal Estuarial and Harbour Engineers' Reference Book.* Oxford: The Alden Press.
- Abreu, T., Silva, P.A., Sancho, F. & Temperville, P. (2010). Analytical approximate wave form for asymmetric waves. *Coastal Engineering, 57*, 656-667. Doi: 10.1016/j.coastaleng.2010.02.005
- Brown, E., Colling, A., Park, D., Phillips, J., Rothery, D. & Wright, J. (2002). *Waves, Tides and Shallow-Water Processes.* Oxford: Butterworth-Heinemann.
- Doering, J.C. & Bowen, A.J. (1995). Parameterization of orbital velocity asymmetries of shoaling and breaking waves using bispectral analysis. *Coastal Engineering, 26*, 15-33. Doi: 10.1016/0378-3839(95)00007-X
- Elfrink, B., Hanes, D.M. & Ruessink, B.G. (2006). Parameterization and simulation of near bed orbital velocities under irregular waves in shallow water. *Coastal Engineering, 53,* 915-927. Doi: 10.1016/j.coastaleng.2006.06.002
- Elgar, S. (1987). Relationships involving third moments and bispectra of a harmonic process. *IEEE Transactions on Acoustics, Speech, and Signal Processing AASP, 35,* 1725-1726. Doi: 10.1109/TASSP.1987.1165090
- Isobe, M. & Horikawa, K. (1982). Study on water particle velocities of shoaling and breaking waves. *Coastal Engineering in Japan, 25*, 109-123
- Malarkey, J. & Davies, A.G. (2012). Free-stream velocity descriptions under waves with skewness and asymmetry. *Coastal Engineering, 68*, 78-95. Doi: 10.1016/j.coastaleng.2012.04.009
- Ruessink, B.G., Michallet, H., Abreu, T., Sancho, F., Van der A, D.A., Van der Werf, J.J. & Silva. P.A. (2011). Observations of velocities, sand concentrations, and fluxes under velocity-asymmetric oscillatory flows. *Journal of Geophysical Research, 116,* C03004. Doi: 10.1029/2010JC006443
- Ruessink, B.G., Raemaekers, G. & van Rijn, L.C. (2012). On the parameterization of the free-stream non-linear wave orbital motion in nearshore morphodynamic models. *Coastal Engineering, 65*, 56-63. Doi: 10.1016/j.coastaleng.2012.03.006
- Van der A, D.A., Ribberink, J.S., Van der Werf, J.J., O'Donoghue, T., Buijsrogge, R.H. & Kranenbrug, W.M. (2013). Practical sand transport formula for non-breaking waves and currents. *Coastal Engineering,* 76, 26-42. Doi: 10.1016/j.coastaleng.2013.01.007

Other sources

- University of Aberdeen. (n.d.). *SINBAD Project. Consulted at 26 March 2015 on:* http://www.abdn.ac.uk/engineering/research/sinbad-project-216.php
- SonTek. (n.d.). *Products. Consulted at 9 June 2015 on:* http://www.sontek.com/productsdetail.php?10-MHz-ADV-2
- Van der A, D.A., Cáceres, I. (2015). *Data Storage Report SINBAD II (Fixed Bed experiments) Canal d'Invesitgació i Experimentació Marítima (CIEM), UPC.*

Appendix

A. Isobe & Horikawa (1982)

Expression for r:	
$r = r_1 - r_2 * \exp^{-\frac{r_3 h}{Los}}$	(A.1)
$r_1 = 1 \; near \; the \; bottom$	(A.2)
$r_2 = 3.2\left(\frac{H_0}{L_0}\right)^{0.65}$	(A.3)
$r_3 = -27 * \log_{10}\left(\frac{H_0}{L_{0s}}\right) - 17$	(A.4)
Expression for $\lambda_{1\text{-}5}$:	
$\lambda_1 = 0.5 - \lambda_3$	(A.5)
$\lambda_2 = \lambda_3\lambda_4 + \lambda_5$	(A.6)
$\lambda_3 = \frac{0.5-\lambda_5}{\lambda_4 - 1 + \exp^{(-\lambda_4)}}$	(A.7)
$\lambda_4 = -15 + 1.35\left(\frac{T}{\sqrt{\frac{g}{h}}}\right) \qquad for \left(\frac{T}{\sqrt{\frac{g}{h}}}\right) \leq 15$	(A.8)
$\lambda_4 = -2.7 + 0.53\left(\frac{T}{\sqrt{\frac{g}{h}}}\right) \qquad for \left(\frac{T}{\sqrt{\frac{g}{h}}}\right) > 15$	(A.9)
$\lambda_5 = 0.0032\left(\frac{T}{\sqrt{\frac{g}{h}}}\right)^2 + 0.000080\left(\frac{T}{\sqrt{\frac{g}{h}}}\right)^3 \qquad for \left(\frac{T}{\sqrt{\frac{g}{h}}}\right) \leq 30$	(A.10)
$\lambda_5 = 0.0056\left(\frac{T}{\sqrt{\frac{g}{h}}}\right)^2 + 0.000040\left(\frac{T}{\sqrt{\frac{g}{h}}}\right)^3 \qquad for \left(\frac{T}{\sqrt{\frac{g}{h}}}\right) > 30$	(A.11)
Expressions for parameters:	
$A = \lambda_1 + \lambda_2\left(\frac{\hat{u}}{\sqrt{gh}}\right) + \lambda_3 * \exp^{-\lambda_4\left(\frac{\hat{u}}{\sqrt{gh}}\right)}$	(A.12)
$B = 0.62 + \frac{0.003}{\beta}$	(A.13)
$C = (1 - \lambda_1) - \lambda_2\left(\frac{\hat{u}}{\sqrt{gh}}\right) - \lambda_3 * \exp^{-\lambda_4\left(\frac{\hat{u}}{\sqrt{gh}}\right)}$	(A.14)
$D = 0.018\left(\frac{T}{\sqrt{\frac{g}{h}}}\right)$	(A.15)
$\theta_1 = \frac{1-\frac{T_c}{T}}{\pi} * \arcsin\left(\sqrt{\frac{\gamma_u^2\gamma_T^2 - 1}{\gamma_u^2(\gamma_T^2 - 1)}}\right) - \theta_2$	(A.16)
$\theta_2 = \frac{\frac{T_c}{T}}{\pi} * arcsin\left(\sqrt{\frac{\gamma_u^2\gamma_T^2 - 1}{\gamma_T^2 - 1}}\right)$	(A.17)
$\gamma_u = \frac{1-\frac{u_c}{\hat{u}}}{\frac{u_c}{\hat{u}}}$	(A.18)
$\gamma_T = \frac{1-\frac{T_c}{T}}{\frac{T_c}{T}}$	(A.19)

B. Elfrink *et al.* (2006)

The rest of the parameterisation of Elfrink *et al.* (2006) is described in this attachment.

Orbital velocity parameters:	
$u_r^E = (H^*)\left(L^{*2}\right)$	(B.1)
$u^* = 2u_2u_w$	(B.2)
$u_{max} = u_1u^*$	(B.3)
$u_t = u^* - u_{max}$	(B.4)
$u_{0c} = \frac{u_{max}T_0 - u_t(1-T_0)}{T_0 - T_1}$	(B.5)
Correction factors for large values of u_{0c}:	
$if\ u_{0c} > 0.25u_{max}\ then\ u_{0c} = 0.25u_{max}$	(B.6)
$a_1 = \frac{-u_t+T_1u_{0c}}{T_0(u_{0c}-u_{max}-u_t)}$	(B.7)
$if\ a_1 < 0.99\ then\ T_0 = 0.99T_0\ and\ u_t = \frac{-(T_0-T_1)u_{0c}+T_0u_{max}}{1-T_0}$	(B.8)
$if\ a_1 \geq 0.99T_0 then\ T_0 = a_1T_0$	(B.9)
Expression for u_1:	
$c_1 = L^* - 10$	(B.10)
$c_2 = \lvert c_1 - (H^* - \lvert\xi\rvert)\rvert$	(B.11)
$c_3 = \xi(1-c_1)$	(B.12)
$c_4 = \tanh\frac{\lvert c_3 - c_2\rvert}{U_r^E}$	(B.13)
$c_5 = \sqrt{\lvert\xi\rvert + \tanh(c_4)}$	(B.14)
$P_1 = \sqrt{H^*} - c_5H^*$	(B.15)
$u_1 = 0.5366P_1 + 0.38989$	(B.16)
Expression for u_2:	
$d_1 = 3\xi + 2\frac{L^*}{U_r^E}$	(B.17)
$d_2 = \sqrt{L^*} - \tanh(\lvert d_1\rvert)$	(B.18)
$d_3 = \left(2\xi + \sqrt{\frac{L^*}{U_r^E}}\right)^2$	(B.19)
$d_4 = U_r + \frac{L}{d_3U_r^E}$	(B.20)
$d_5 = \sqrt{\frac{d_2}{d_4}}$	(B.21)
$P_2 = 1.2001d_5 + 0.4758$	(B.22)
$u_2 = 1.1600P_2 - 0.0145$	(B.23)
Expression for T_1:	
$e_1 = H^*L^*\xi$	(B.24)
$e_2 = e_1(-9.8496\xi H^*)^2$	(B.25)
$e_3 = \tanh(e_2) + \tanh(e_1) + L^* - 1$	(B.26)
$P_3 = \tanh\left(-\frac{9.3852}{e_3}\right)$	(B.27)
$T_1 = -0.2615P_3 - 0.0005$	(B.28)
Expression for T_0:	
$f_1 = 0.0113\,\xi L^{*2}$	(B.29)

$f_2 = 3.5667 * 10^{-4} \xi L^{*4}$	(B.30)
$f_3 = 0.1206 L^* * \tanh(tanh(\xi))$	(B.31)
$f_4 = H^* \dfrac{\tanh(f_2)}{\tanh(f_3)}$	(B.32)
$P_4 = H^* * \tanh\big(0.02899 L^*(f_1)\big) - \tanh(f_4)$	(B.33)
$T_0 = 0.0958 P_4 + 0.5028$	(B.34)
Expression for T_2:	
$g_1 = \xi + 0.9206$	(B.35)
$g_2 = L^* - \sqrt{U_r^E} + \sqrt{\dfrac{2.5185}{L^*}} - 4.6505$	(B.36)
$g_3 = \sqrt{\left\lvert \dfrac{g_2}{H^*} \right\rvert}$	(B.37)
$g_4 = \lvert L^* + \xi \rvert - 4.4995 + \xi$	(B.38)
$g_5 = \lvert g_4 + \lvert \xi \rvert - 5.3981 \rvert$	(B.39)
$g_6 = \left\lvert L^* + \sqrt{\dfrac{3.0176}{H^*}} - 5.2868 + H^* \right\rvert$	(B.40)
$g_7 = \lvert \xi + 0.1950(g_6 + \xi) \rvert$	(B.41)
$g_8 = \lvert \xi \rvert + L^*$	(B.42)
$P_5 = \dfrac{4.1958}{g_1 + g_3 + g_5 + g_7 + g_8}$	(B.43)
$T_2 = -0.5623 P_5 + 0.9209$	(B.44)

C. Smoothened and non-smoothened measured free-stream velocities

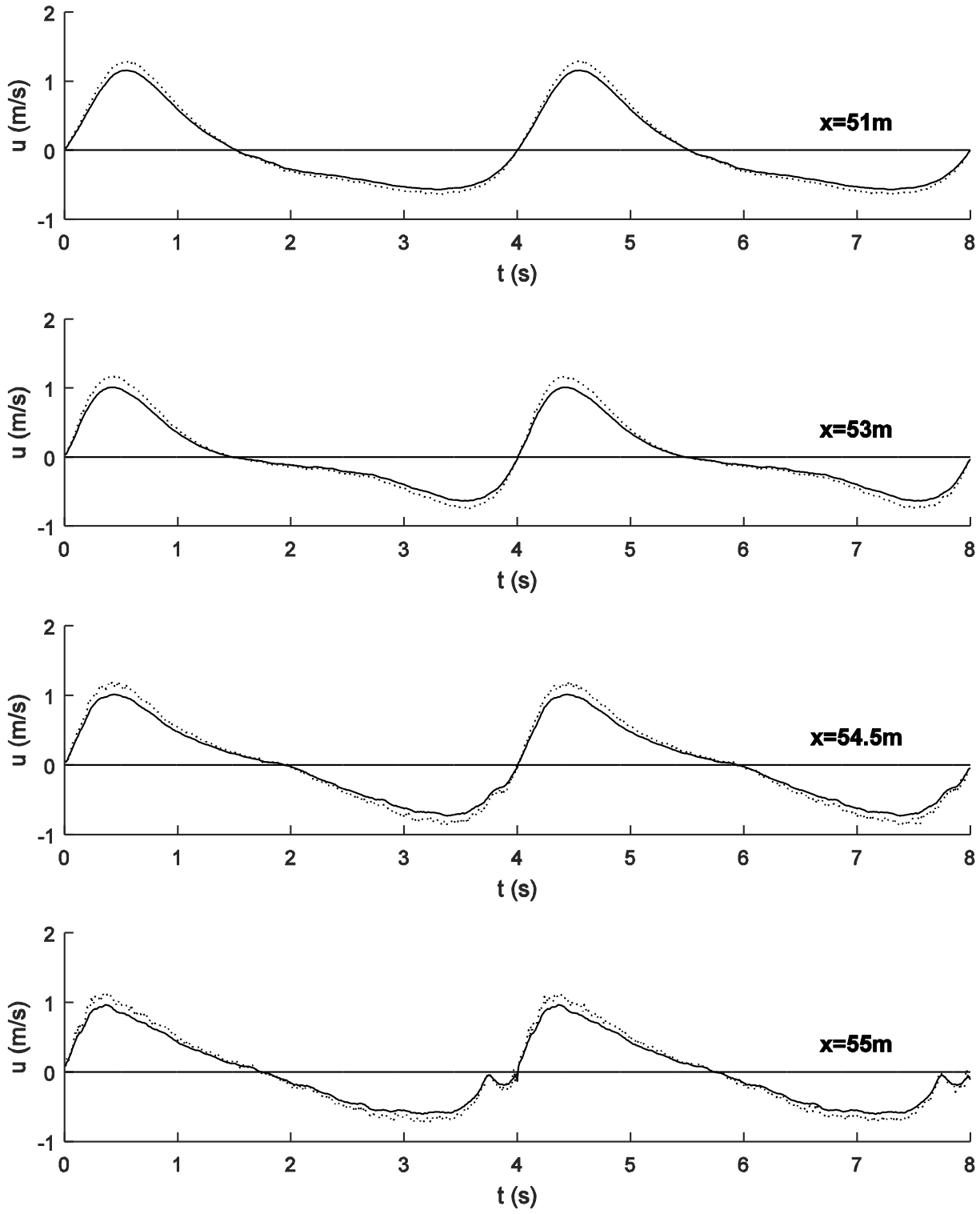

Figure C.1: Smoothened (solid line) and non-smoothened (dotted line) measured free-stream velocity time series for four locations between x=51m and x=55m

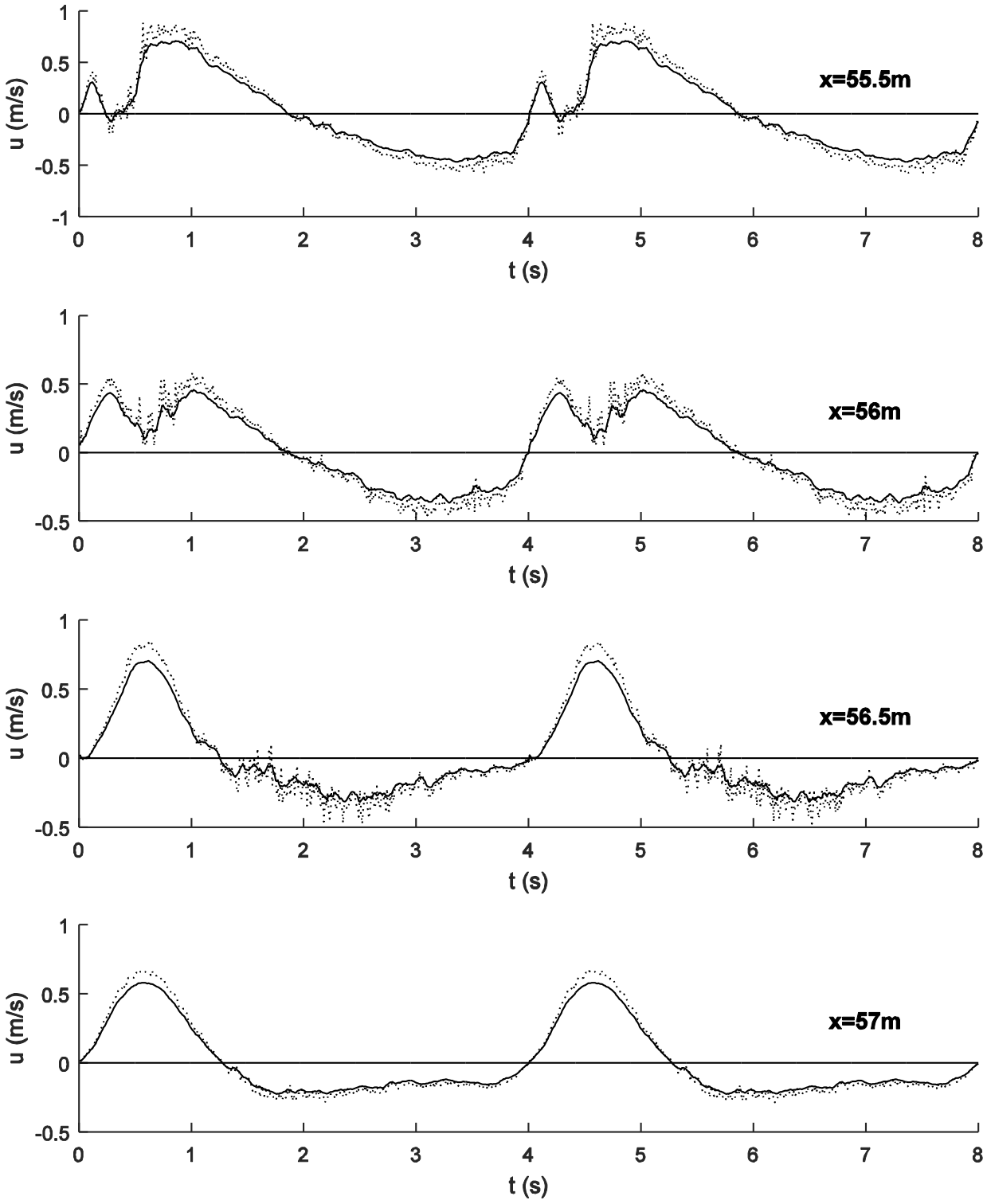

Figure C.2: Smoothened (solid line) and non-smoothened (dotted line) measured free-stream velocity time series for four locations between x=55.5m and x=57m

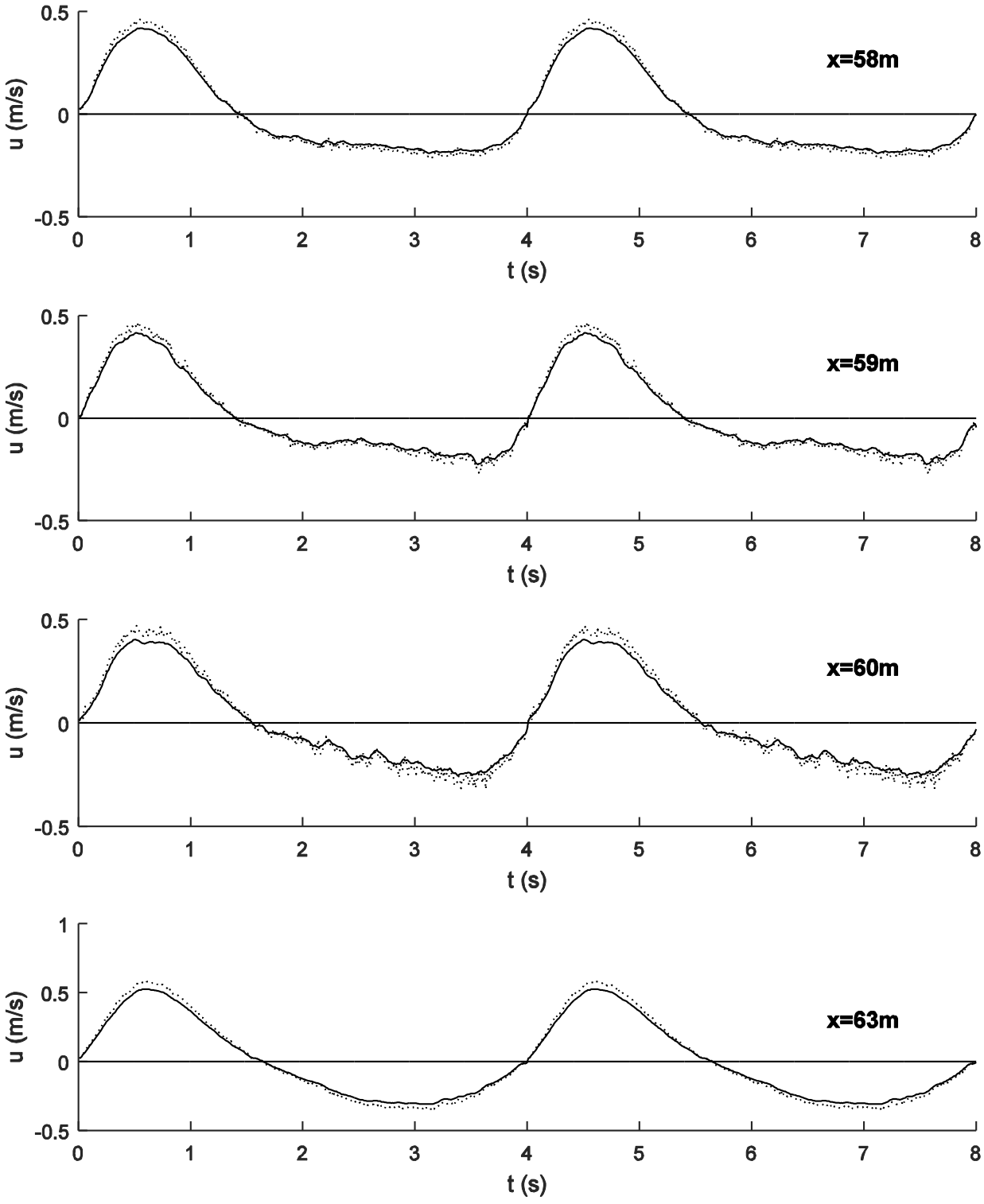

Figure C.3: Smoothened (solid line) and non-smoothened (dotted line) measured free-stream velocity time series for four locations between x=58m and x=63m

D. Velocity time series before and after removing the undertow

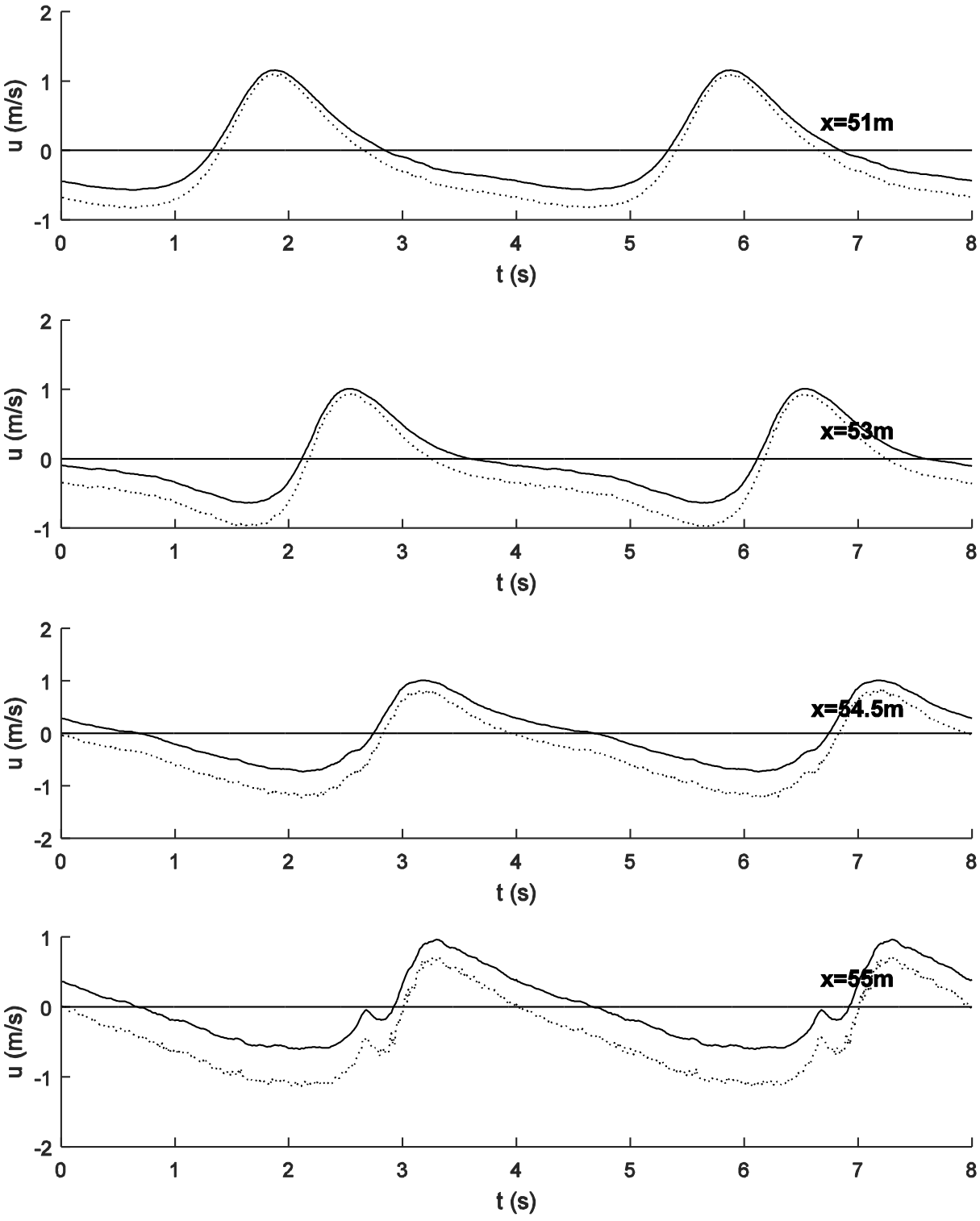

Figure D.1: solid line: velocity time series with the undertow removed, dotted line: velocity time series with undertow, for four locations between x=51m and x=55m

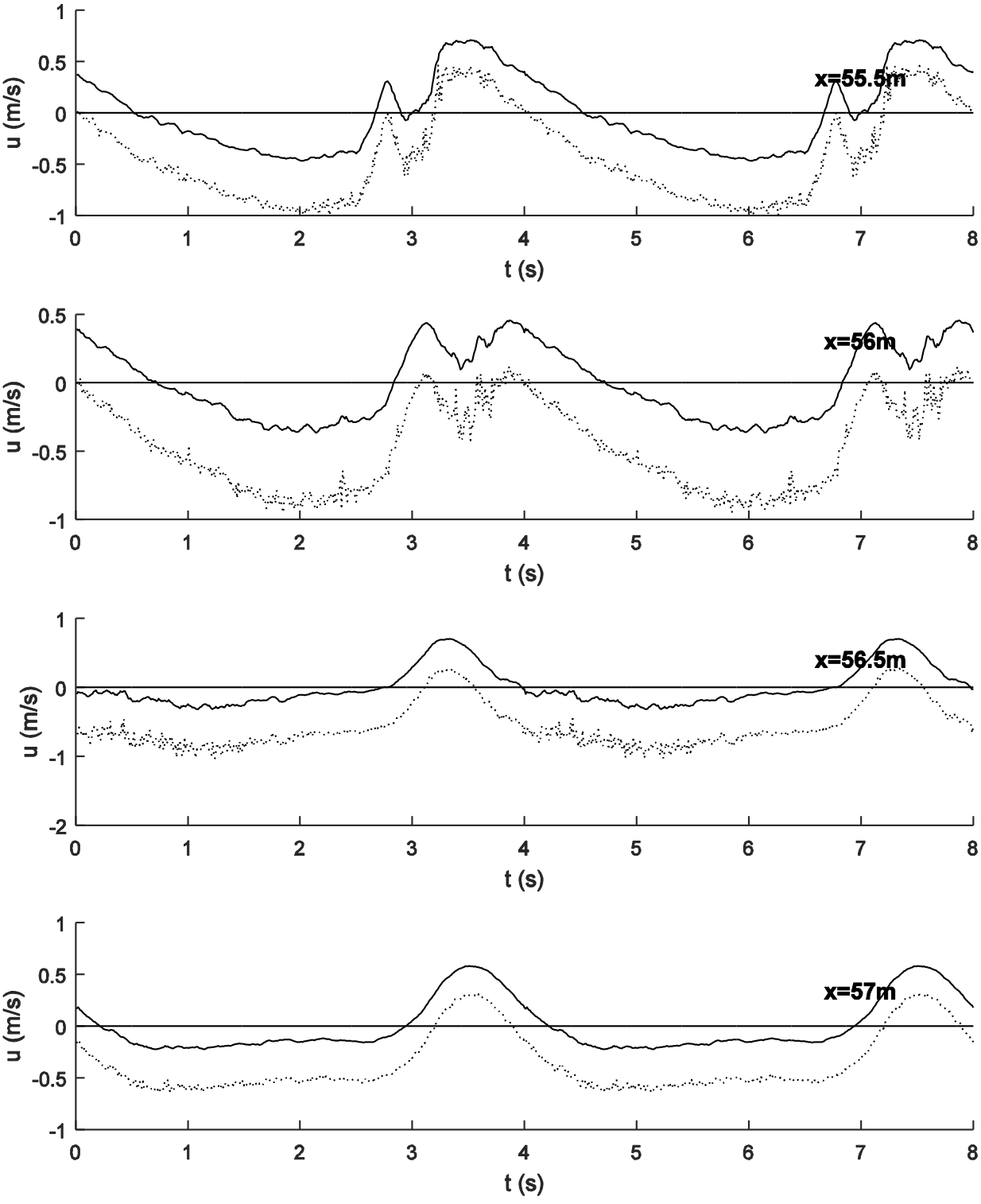

Figure D.2: solid line: velocity time series with the undertow removed, dotted line: velocity time series with undertow, for four locations between x=55.5m and x=57m

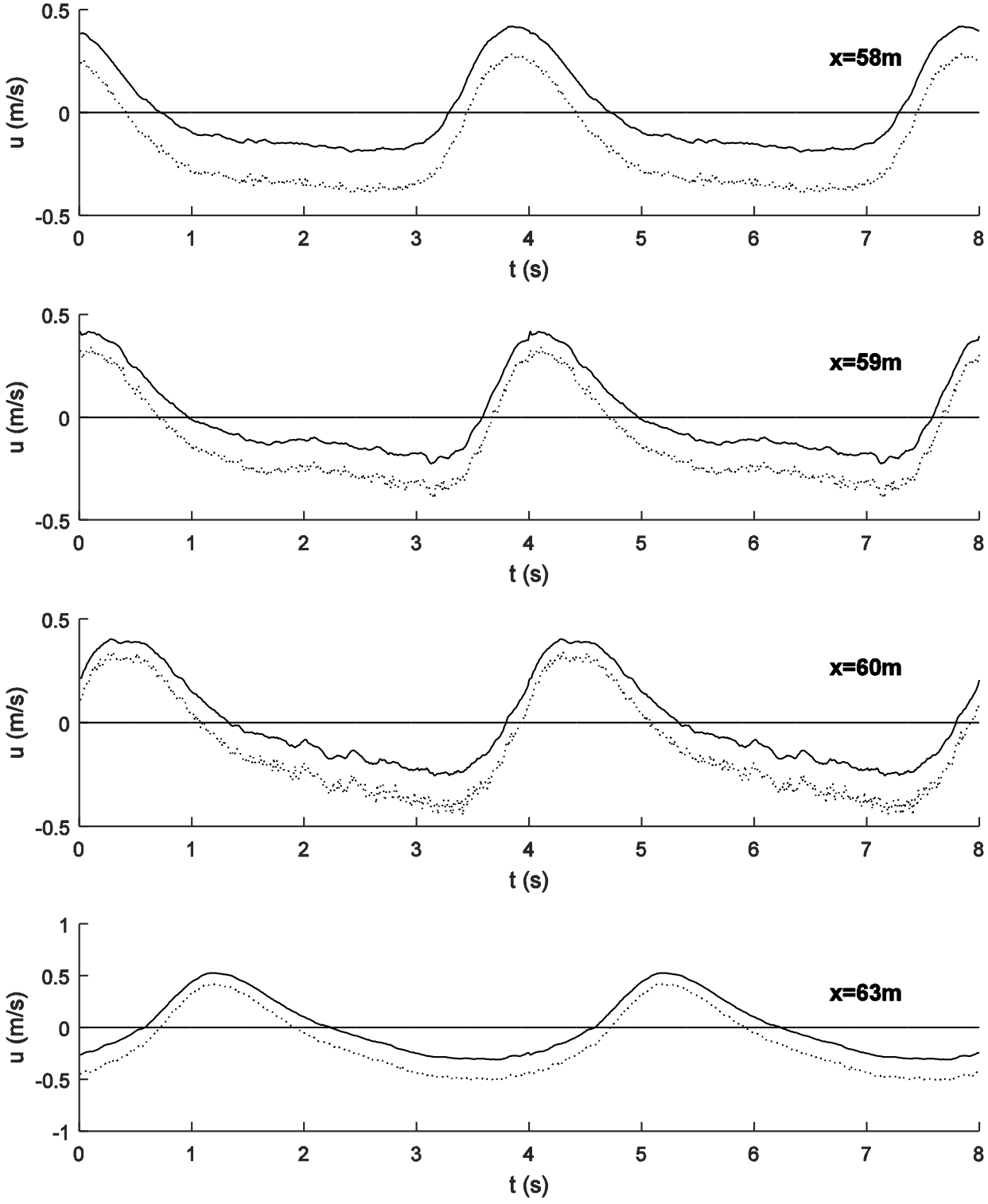

Figure D.3: solid line: velocity time series with the undertow removed, dotted line: velocity time series with undertow, for four locations between x=58m and x=63m

E. Acceleration time series

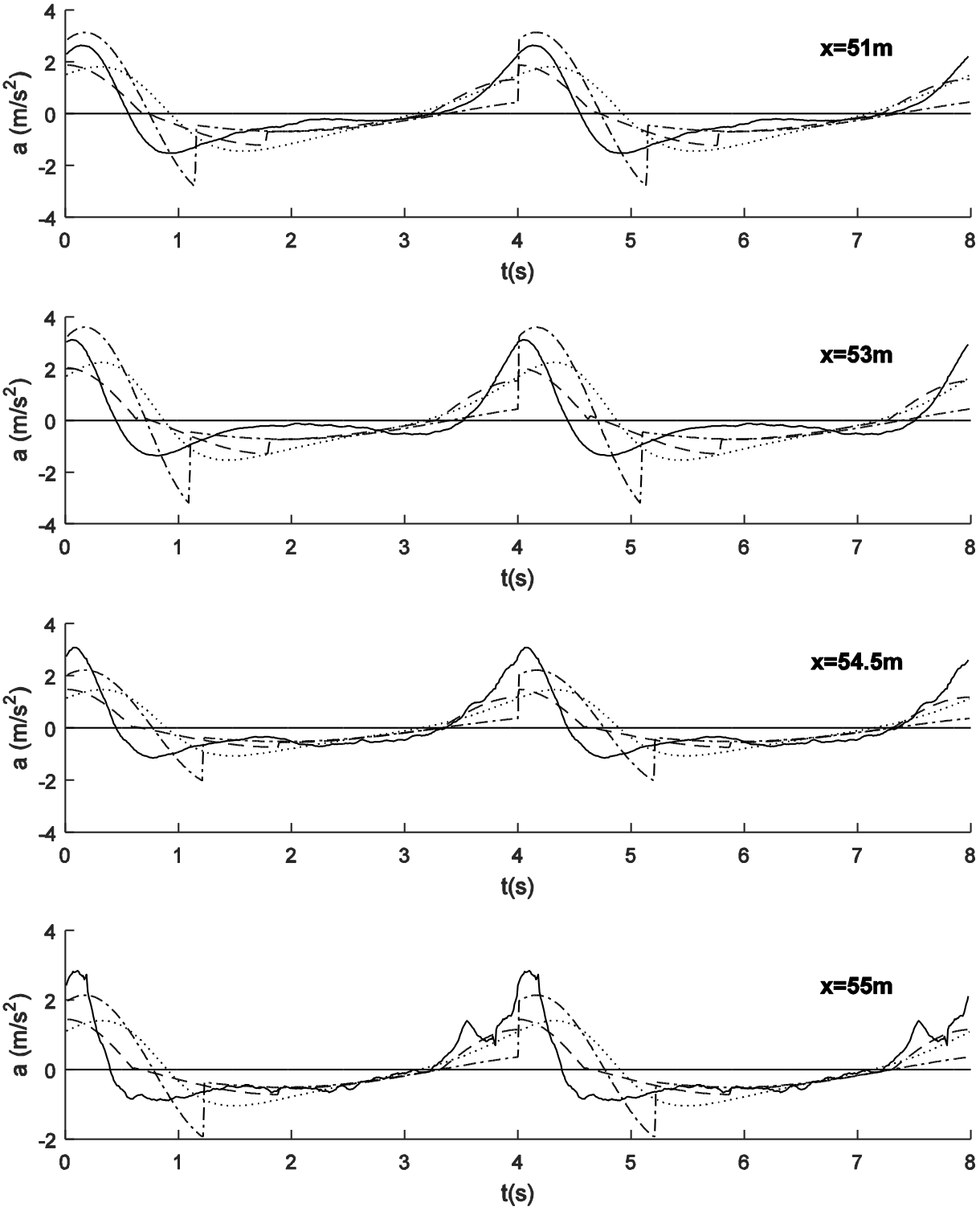

Figure E.1: Measured and computed acceleration time series, for four locations between x=51m and x=55m, solid line: measured velocities, dash-dotted: Isobe & Horikawa (1982), dashed line: Elfrink *et al.* (2006), dotted line: Ruessink *et al.* (2012)

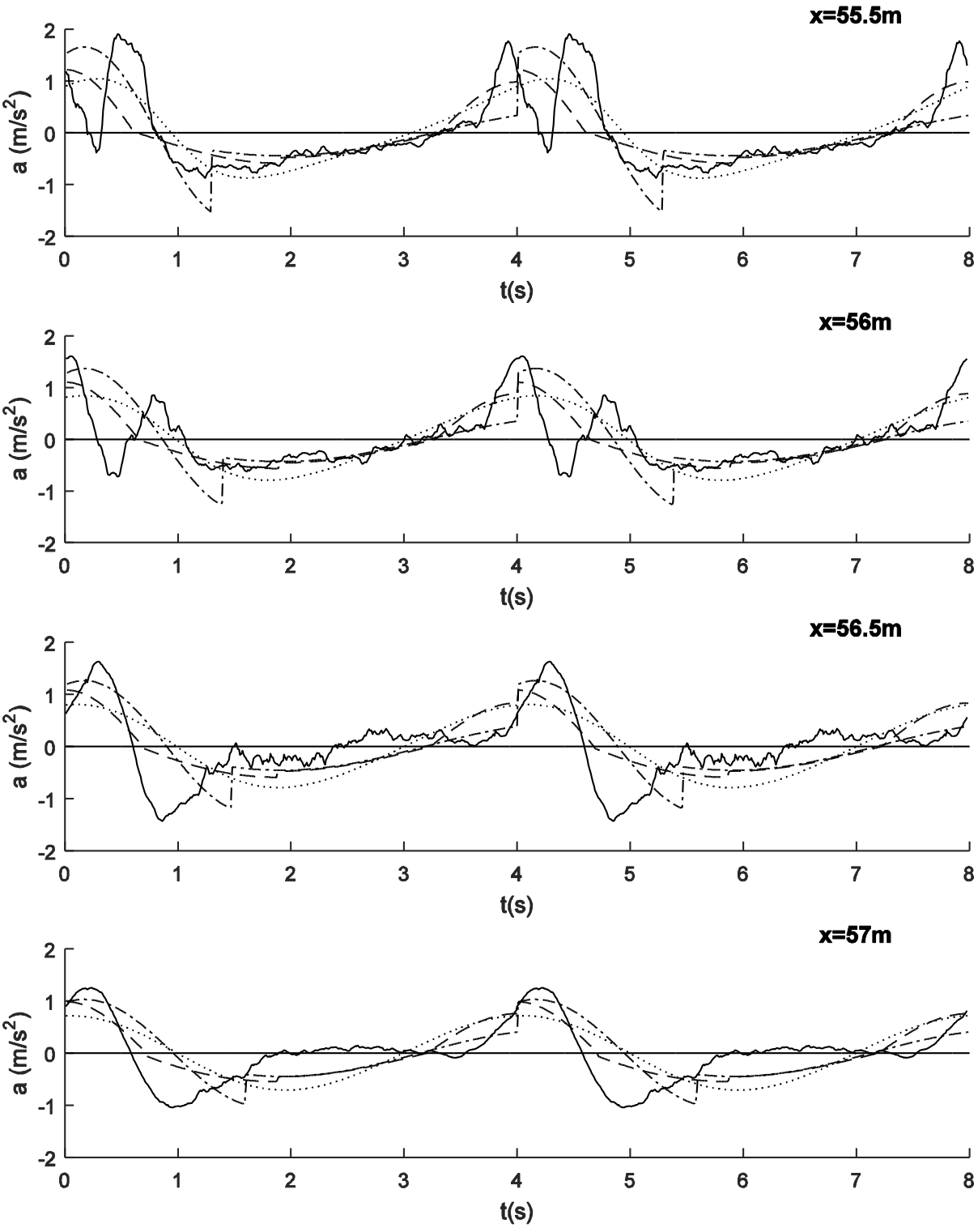

Figure E.2: Measured and computed acceleration time series, for four locations between x=55.5m and x=57m, solid line: measured velocities, dash-dotted: Isobe & Horikawa (1982), dashed line: Elfrink *et al.* (2006), dotted line: Ruessink *et al.* (2012)

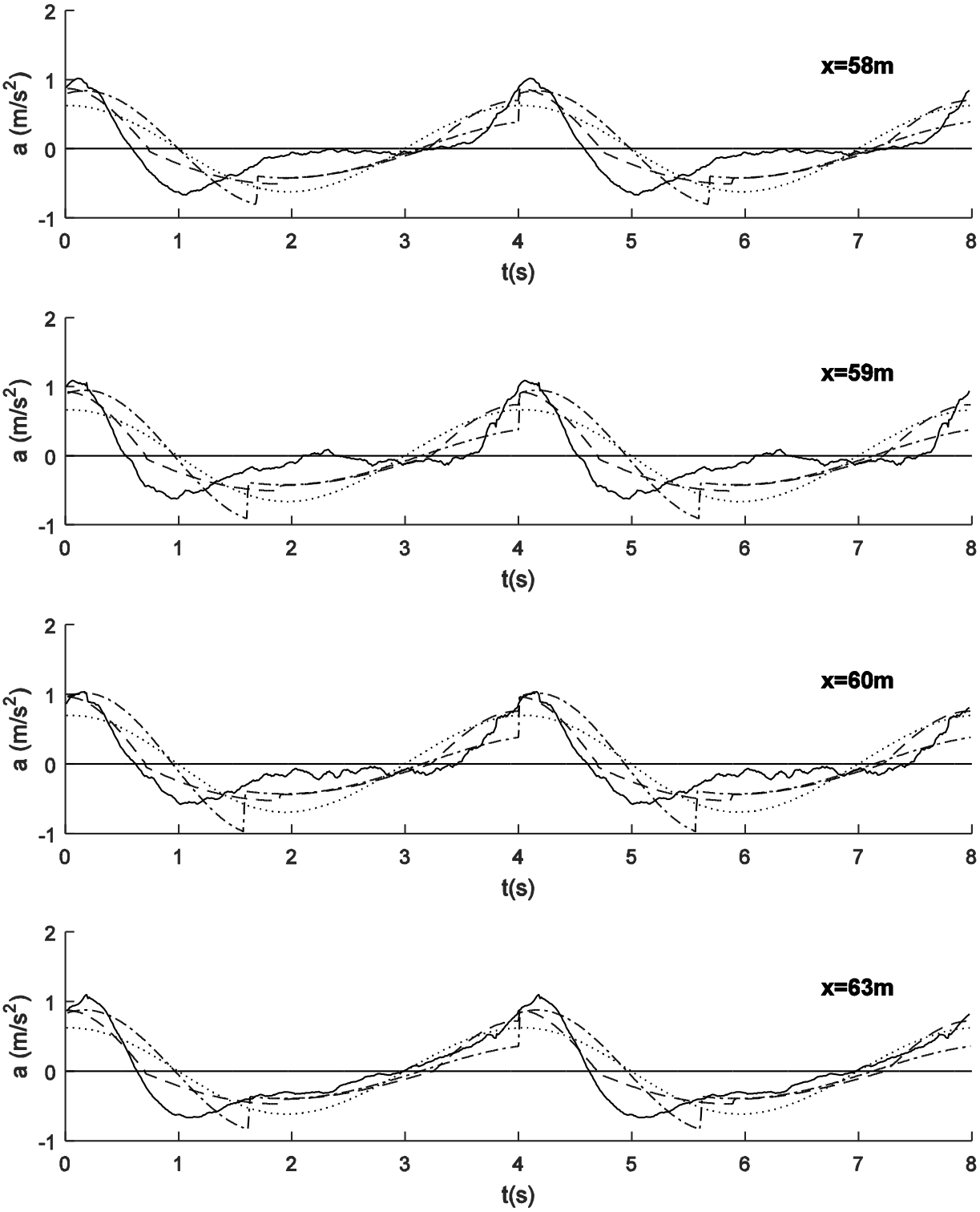

Figure E.3: Measured and computed acceleration time series, for four locations between x=58m and x=63m, solid line: measured velocities, dash-dotted: Isobe & Horikawa (1982), dashed line: Elfrink *et al.* (2006), dotted line: Ruessink *et al.* (2012)